December 1999

UILU-ENG-99-2233
DC-192

University of Illinois at Urbana-Champaign

Achieving Nonvanishing Stability Regions with High-Gain Cheap Control Using H∞ Techniques: The Second Order Case

Gregory J. Toussaint and Tamer Başar

Coordinated Science Laboratory
1308 West Main Street, Urbana, IL 61801

SF 298 MASTER COPY KEEP THIS COPY FOR REPRODUCTION PURPOSES

REPORT DOCUMENTATION PAGE

Form Approved
OMB NO. 0704-0188

1. AGENCY USE ONLY *(Leave blank)*	2. REPORT DATE	3. REPORT TYPE AND DATES COVERED
	December 29, 1999	

4. TITLE AND SUBTITLE
Achieving Nonvanishing Stability Regions with High-Gain Cheap Control Using H^∞ Techniques: The Second Order Case

5. FUNDING NUMBERS

6. AUTHOR(S)
Gregory J. Toussaint and Tamer Başar

7. PERFORMING ORGANIZATION NAMES(S) AND ADDRESS(ES)
Coordinated Science Laboratory
University of Illinois at Urbana-Champaign
1308 West Main Street
Urbana, Illinois 61801-2307

8. PERFORMING ORGANIZATION REPORT NUMBER
UILU-ENG-99-2233
DC-192

9. SPONSORING / MONITORING AGENCY NAME(S) AND ADDRESS(ES)
Department of Energy
Washington, DC

10. SPONSORING / MONITORING AGENCY REPORT NUMBER

11. SUPPLEMENTARY NOTES
The views, opinions and/or findings contained in this report are those of the author(s) and should not be construed as an official position, policy or decision, unless so designated by other documentation.

12a. DISTRIBUTION / AVAILABILITY STATEMENT
Approved for public release; distribution unlimited.

12 b. DISTRIBUTION CODE

13. ABSTRACT *(Maximum 200 words)*

We demonstrate how to use an asymptotically optimal H-infinity optimal disturbance attenuation controller to stabilize a second-order system subject to unknown disturbances such that the stability region does not vanish as the feedback gains increase. The high-gain feedback arises when we try to approach the disturbance attenuation lower limit of the H-infinity design. This type of gain increase can cause the stability region to vanish if the disturbance contains nonlinear terms. Our analysis using Lyapunov techniques derives a sufficient condition on the design parameters to prevent the stability region from vanishing. The high-gain techniques create a two time-scale behavior in the system response which is similar to the response from a singularly perturbed system. In addition to finding exact solutions for six different cases, we provide simulations to illustrate the results for a second-order.

14. SUBJECT TERMS
Stability domains, High-gain feedback, Cheap control, H-infinity control and Disturbance rejection

15. NUMBER IF PAGES

16. PRICE CODE

17. SECURITY CLASSIFICATION OR REPORT	18. SECURITY CLASSIFICATION OF THIS PAGE	19. SECURITY CLASSIFICATION OF ABSTRACT	20. LIMITATION OF ABSTRACT
UNCLASSIFIED	UNCLASSIFIED	UNCLASSIFIED	UL

Achieving Nonvanishing Stability Regions with High-Gain Cheap Control Using H^∞ Techniques: The Second Order Case*

Gregory J. Toussaint Tamer Başar

Coordinated Science Laboratory and
Department of Electrical and Computer Engineering
University of Illinois at Urbana-Champaign
1308 West Main Street
Urbana, IL 61801

December 10, 1999

Abstract

We demonstrate how to use an asymptotically optimal H^∞-optimal disturbance attenuation controller to stabilize a second-order system subject to unknown disturbances such that the stability region does not vanish as the feedback gains increase. The high-gain feedback arises when we try to approach the disturbance attenuation lower limit of the H^∞ design. This type of gain increase can cause the stability region to vanish if the disturbance contains nonlinear terms. Our analysis using Lyapunov techniques derives a sufficient condition on the design parameters to prevent the stability region from vanishing. The high-gain techniques create a two time-scale behavior in the system response which is similar to the response from a singularly perturbed system. In addition to finding exact solutions for six different cases, we provide simulations to illustrate the results for a second-order system.

1 Introduction

In simple terms, the stability region of a system is the set of initial conditions that lead to a stable response for the system. The problem of describing the stability region for a dynamical system has been studied at length for a variety of applications including electrical power systems, economics, chemical reactions and ecology [1]. The importance of this problem has led to numerous techniques for estimating the stability region, (which is also known as the region of attraction). Genesio, Tartaglia and Vicino [2] provide a comprehensive summary of the basic approaches for determining the stability region and offer their own numerical approach. Their technique is based on reversing the system trajectories and is also described by Genesio and Vicino in [3]. Chiang and Thorp detail an iterative method using Lyapunov functions to monotonically improve the stability region estimate [1]. Chiang and Fekih extend this method and specialize it to interconnected nonlinear systems in [4]. Another algorithm by Chiang, Hirsch and Wu [5] determines the exact stability region under certain conditions by finding the union of the stable manifolds of the equilibrium points. More recently, Chiang and Fekih [6] have considered quasi-stability regions as a close approximation to the original goal. All of this literature is a fraction of that available on the subject, which confirms that stability region estimation is a fundamental problem in system analysis.

Having solved the problem of finding the stability region for several cases using an assortment of techniques, one logical extension is to examine the behavior of the region under different conditions. Here we focus on one condition that causes the stability region to vanish and how to compensate for it. The condition

*Research supported in part by the U. S. Department of Energy under Grant DE-FG-02-97-ER-13939.

of interest is high-gain linear feedback arising from an optimal H^∞ design, when also the cost on control vanishes.

The H^∞ design approach allows us to ensure that a given level of disturbance attenuation is achieved. Using standard results on H^∞-optimal control [7], if we choose to push the design toward the lower bound on the attenuation level, then this will dictate an increase in the feedback gains. This high-gain linear feedback offers a variety of advantages when controlling linear systems with unknown disturbances. As described in [8], such designs feature a fast response, good disturbance rejection and insensitivity to parameter variations. These benefits may come with a price: if we neglect the possibly nonlinear disturbances, then we may create a vanishing stability region as the feedback gains increase. With a small stability region, the system to be controlled would require only a minor perturbation to generate an unbounded response. Even if we design an optimal controller in the H^∞ sense, the resulting system would be unacceptable, if the stability region is vanishingly small.

Kokotović and Marino [8] document the effects on the stability region of increasing feedback gains for three second-order systems with nonlinear disturbances. In each case, using the linear feedback control law

$$u = -k_1 x_1 - k_2 x_2, \qquad k_1 = k_2^2, \tag{1}$$

caused the system's stability region to vanish as the gain increased. Kokotović and Marino describe how to use feedback linearization to resolve this problem when the system satisfies certain conditions. Although feedback linearization successfully addresses the problem, it may eliminate a potentially beneficial nonlinear term in the system which improves the overall stability properties. See dAndrea and Levine [9] for a related discussion of exact linearization and high-gain feedback with applications to robotics.

In the semi-global stabilization methods of [10], Teel and Praly develop high-gain controllers that lead to nonvanishing stability regions for unknown but bounded disturbances. In the second-order case, they produce linear feedback controllers with the property that

$$k_1 = k_2^n, \qquad n < 2. \tag{2}$$

Their solution offers one approach for stabilizing the system and maintaining the stability region, but they do not use the H^∞ framework in their analysis. Krstić, Sun and Kokotović [11] consider and solve a similar problem with input unmodeled dynamics. Their approach to achieve global asymptotic stability uses a dynamic nonlinear damping design. They extend the results to higher-order systems using a recursive integrator backstepping technique.

Our approach to designing a stabilizing controller contributes to the existing research by looking at the problem from an H^∞ perspective. We want to use the power of H^∞-optimal design methods to develop linear feedback control laws to stabilize systems with bounded disturbances. Simultaneously, we want to ensure the stability region for the feedback system does not vanish as the gain is increased and the optimal attenuation level is approached. We will formally state this problem and provide a solution, including simulations, for a second-order system.

Although not the primary intent of this paper, our solution to the problem reveals a two time-scale behavior in the resulting system dynamics. The behavior arises because the feedback gains approach infinity at different rates. Past research has discussed a wide range of techniques for controlling such systems. Chow and Kokotović [12] outline a procedure to analyze a system with slow and fast modes and design a composite regulator that approximates the optimal performance. Saberi and Khalil [13] extend the above technique to nonlinear systems and Khalil [14] addresses a similar problem for nonlinear, multiparameter singularly perturbed systems. Cheung and Chow [15] use the slow and fast manifold of a singularly perturbed system to estimate the stability region of the system. Recently, and germane to our discussion, Pan and Başar [16, 17] have combined the techniques from [12] with H^∞ design using a differential game theoretical approach. These approaches to studying the stability region and controlling systems with two time-scale behavior offer reasonable alternatives for the basic approach we employ.

We will proceed as follows. In Section 2, we define a second-order version of the problem and use the H^∞-optimal disturbance attenuation approach (from [7]) with cheap control to produce high-gain controllers. We will describe parameter choices for our design that let the system approach the optimal attenuation level and drive the gains to infinity. The method will allow for some selection of the rates and relative rate at which the closed-loop eigenvalues increase and also allows for selection of the parameter n in (2).

After we show how to construct a high-gain linear feedback controller using an H^∞ approach, in Section 3 we will build on these results by applying Lyapunov techniques to the second-order high-gain case [18]. We will develop a sufficient condition for the parameter n to ensure a nonvanishing stability region as the gains increase. Our analysis depends on the disturbance having a restricted form and on knowing a bound on the nonlinear disturbance.

In Section 4, we present an example and simulate a second-order system for three different values of n to show how the method can lead to nonvanishing stability regions. The simulation highlights the fact that our conditions on n are only sufficient, since violating the conditions does not always lead to vanishing stability regions. These results make sense given the Lyapunov-based design we used to describe the stability region.

Finally, Section 5 provides a summary, concluding comments and possible extensions to the current effort. The three appendices provide the derivations and numerical details for some of the main results.

2 Problem Formulation and Solutions

We begin by describing the system we will focus on and by solving the H^∞ problem associated with it. We will also explore the conditions that must be satisfied to find a valid solution and the behavior of the closed-loop system as the feedback gains increase. There are six variations of the original set of parameters, so we will examine one in detail and just state the results for the others. The appendices provide the details omitted here.

For the basic system we consider a double integrator with disturbances, described by

$$\dot{x} = Ax + Bu + Dw, \tag{3}$$

where,

$$A = \begin{pmatrix} 0 & 1 \\ 0 & 0 \end{pmatrix}, \quad B = \begin{pmatrix} 0 \\ 1 \end{pmatrix}, \quad D = \begin{pmatrix} 1 & 0 \\ 0 & 1 \end{pmatrix}.$$

The state vector is $x \in \mathbb{R}^2$, the state feedback control input is $u \in \mathbb{R}$ and the disturbance is $w \in \mathbb{R}^2$. Certain nonlinear systems can be transformed into a chain of integrators, similar to this system, by feedback linearization (as in [19, 18]). If the costs used to evaluate the system are in a quadratic form or if we can transform them into a quadratic form, then H^∞ techniques and the following results may be useful in controlling such systems.

Using standard notation, we can describe disturbance attenuation with the functional J, defined as

$$J := \sqrt{\frac{\|x\|_Q^2 + \|u\|_R^2}{\|w\|^2}}, \tag{4}$$

where

$$\|x\|_Q^2 := \int_0^\infty x^T(t) Q x(t)\, dt,$$

and

$$Q = \begin{pmatrix} q_1 & 0 \\ 0 & q_2 \end{pmatrix}, \quad q_1 > 0, \quad q_2 \geq 0, \quad R = \varepsilon^2 > 0.$$

The parameter R determines the cost on the control input u. Since we will allow ε to approach zero, R will tend to be small and the control cost will be cheap. This cheap control is one way of guaranteeing achievement of the high-gain feedback we want to examine.

With u taken as a state feedback controller, we define γ^* as

$$\gamma^* := \min_u \max_w J, \tag{5}$$

which is the minimax (optimal) attenuation level the system can achieve. Since (A, B) is controllable and (A, Q) is observable, $\gamma^* < \infty$, and for all $\gamma > \gamma^*$ the generalized algebraic Riccati equation (GARE)

$$A^T Z + ZA - Z(BR^{-1}B^T - \frac{1}{\gamma^2}DD^T)Z + Q \;=\; 0, \tag{6}$$

has a minimal positive definite solution for the matrix Z [7], and for the two dimensional system above, since A has no stable eigenvalues, (6) has exactly one positive definite and one negative definite solution. Thus, for every $\gamma > \gamma^*$ we can achieve a disturbance attenuation level at least as good as γ by solving for the unique positive definite solution Z in (6) and using the linear state feedback

$$u \;=\; -R^{-1}B^T Z\, x(t) \;=\; -\frac{1}{\varepsilon^2}(z_{12}\, x_1 + z_{22}\, x_2), \tag{7}$$

where z_{ij} stands for the ij-th entry of the matrix Z. As an additional result, the closed-loop system matrix, $A - BR^{-1}B^T Z$, will be Hurwitz. On the other hand, if $\gamma < \gamma^*$ in (6), then there is no real solution for Z that leads to a stable closed-loop system.

One of the key steps in our solution to this control problem will be to determine the value of γ^* for the system. The parameter γ^* corresponds to the smallest[1] value of γ that makes Z the unique positive definite solution of (6). Once we know γ^*, we can use a γ that is greater than γ^* and have a stable closed-loop system. Since we are examining a second-order system, we can find an exact solution for γ^* from (6). For a complete discussion of the theory associated with this analysis, see [7].

To proceed with the solution to our problem, we let

$$\beta_1 \;=\; \frac{1}{\gamma^2}, \qquad \beta_2 \;=\; \frac{\gamma^2 - \varepsilon^2}{\gamma^2 \varepsilon^2},$$

to simplify the following expressions from solving (6) for the entries of $Z = \begin{pmatrix} z_{11} & z_{12} \\ z_{12} & z_{22} \end{pmatrix}$:

$$z_{11} \;=\; \left(\frac{\beta_2\, z_{12}^2 - q_1}{\beta_1}\right)^{\frac{1}{2}}, \qquad z_{22} \;=\; \left(\frac{q_2 + 2z_{12} + \beta_1\, z_{12}^2}{\beta_2}\right)^{\frac{1}{2}} \tag{8}$$

with

$$z_{12} \;=\; \frac{\gamma^2 \varepsilon \left[q_1\, \varepsilon + \left(q_1\, [\gamma^2 - q_2]\, [\gamma^2 - \varepsilon^2]\right)^{\frac{1}{2}}\right]}{\gamma^4 - (q_2 + \varepsilon^2)\, \gamma^2 + (q_2 - q_1)\, \varepsilon^2}. \tag{9}$$

For a valid solution we must have a real, positive definite Z matrix, which is equivalent to the following conditions being satisfied:

$$\beta_2\, z_{12}^2 - q_1 \;>\; 0 \tag{10}$$

$$2\beta_2\, z_{12}^3 + (\beta_2\, q_2 - \beta_1\, q_1)\, z_{12}^2 - 2q_1\, z_{12} - q_1\, q_2 \;>\; 0. \tag{11}$$

Condition (10) comes from making z_{11} real (and positive) and condition (11) comes from ensuring $z_{11}\, z_{22} - z_{12}^2 > 0$. In addition to satisfying these two conditions, we must ensure that z_{12} and z_{22} are real. To address all of these requirements, we will first solve for the largest value of γ that makes the denominator of z_{12} zero. Call this value $\bar{\gamma}$. Next, we will show how $\bar{\gamma}$ satisfies all of the conditions and will explain why $\bar{\gamma}$ actually equals γ^*.

Consider the denominator of z_{12} in (9) as a quadratic in terms of γ^2 (i.e., $a\,\gamma^4 + b\,\gamma^2 + c = 0$), solve for the larger root and then take the positive square root of the result to get

$$\bar{\gamma} \;:=\; \frac{1}{\sqrt{2}} \left[q_2 + \varepsilon^2 + (q_2^2 - 2q_2\, \varepsilon^2 + \varepsilon^4 + 4q_1\, \varepsilon^2)^{\frac{1}{2}}\right]^{\frac{1}{2}}. \tag{12}$$

[1]Technically, γ^* is the infimum of the set of values of γ such that the GARE (6) has a positive definite solution.

Suppose we always choose $\gamma > \bar{\gamma}$. Then the denominator of z_{12} will always be positive. This choice will make the argument of the square root in z_{12} positive since

$$(\gamma^2 - q_2)(\gamma^2 - \varepsilon^2) \;=\; \gamma^4 - (q_2 + \varepsilon^2)\,\gamma^2 + q_2\,\varepsilon^2. \tag{13}$$

In (13), the left hand side is a portion of the argument of the square root in z_{12} and the right hand side is always greater than the denominator of z_{12}. Since we selected γ to make the right hand side positive and we must choose $q_1 > 0$, the argument of the square root in (9) is also positive. We can then conclude that z_{12} will always be positive and real.

As γ decreases to $\bar{\gamma}$, the denominator of z_{12} approaches zero, the numerator remains positive and the value of z_{12} approaches infinity. We now choose ε small enough to make β_2 positive (which is always possible) and we note that β_1 is positive. For this fixed value of ε, as z_{12} approaches infinity, conditions (10) and (11) are satisfied, because z_{12} is the dominate factor in both expressions. Also with this value for ε, from (8) we see that z_{22} will be real for large values of z_{12}. We have thus successfully demonstrated that for any $\gamma > \bar{\gamma}$ we satisfy conditions (10) and (11) and we also have real solutions for z_{12} and z_{22}. Now we must explain how $\bar{\gamma}$ is also the optimal disturbance attenuation level.

We have already noted that as γ approaches $\bar{\gamma}$ from above, the value of z_{12} approaches infinity. From (8) we see that both z_{11} and z_{22} grow at rates proportional to z_{12}, so they will also approach infinity as γ decreases to $\bar{\gamma}$. Our analysis above shows the matrix Z remains positive definite as z_{12} increases, but if we allow $\gamma = \bar{\gamma}$, then the entries of Z are not defined and we no longer have a solution to (6). Therefore, $\bar{\gamma}$ is the infimum of values for γ that allow a well-defined, positive definite solution for Z. Since the value of γ^* is unique for this system, we can now conclude that, by definition, $\bar{\gamma} = \gamma^*$.

To quantify our analysis as we allow γ to approach γ^*, we introduce a function $p(\varepsilon) = \varepsilon^c$, for $c > 0$, which represents the difference between γ^2 and γ^{*2}:

$$\gamma^2 \;=\; \gamma^{*2} + p(\varepsilon), \tag{14}$$

and let ε approach zero. Since γ^{*2} is dependent on ε, we must make sure that

$$\lim_{\varepsilon \to 0} \frac{p(\varepsilon)}{\gamma^{*2}} \;=\; 0$$

for γ^2 to approach γ^{*2}. Appendix A shows how this condition is satisfied for all of the parameter variations we encounter. In addition, our simulations will verify this result. Using (14) to substitute for γ^2, we can write the denominator of z_{12} as

$$[\gamma^{*2} + p(\varepsilon)]^2 - [q_2 + \varepsilon^2][\gamma^{*2} + p(\varepsilon)] + [q_2 - q_1]\,\varepsilon^2 \;=$$

$$\gamma^{*4} + 2\gamma^{*2}\,p(\varepsilon) + p^2(\varepsilon) - [q_2 + \varepsilon^2][\gamma^{*2} + p(\varepsilon)] + [q_2 - q_1]\,\varepsilon^2,$$

which becomes

$$2\gamma^{*2}\,p(\varepsilon) + p^2(\varepsilon) - [q_2 + \varepsilon^2]\,p(\varepsilon),$$

after cancelling the terms that add to zero from the definition of $\bar{\gamma} = \gamma^*$.

In our analyses, we restrict q_1 to be a positive constant, but we will study several different options for the parameter q_2. Specifically, we will examine q_2 when it is a positive constant, zero or a positive function dependent on ε. Consider the case where q_2 is a positive constant and $p(\varepsilon) = \varepsilon^c \ll \varepsilon^2$ as ε approaches zero (that is, $c > 2$). We will refer to this set of parameter choices as Case 1. Appendix B.1 provides the derivation to show

$$z_{11} \;\sim\; \frac{2q_1\,\varepsilon\,\sqrt{q_2}}{p(\varepsilon)}, \qquad z_{12} \;\sim\; \frac{2q_1\,\varepsilon^2}{p(\varepsilon)}, \qquad z_{22} \;\sim\; \frac{2q_1\,\varepsilon^3}{p(\varepsilon)\,\sqrt{q_2}},$$

as ε approaches zero. Using (7) we can calculate the feedback gains as

$$k_1 \;=\; \frac{1}{\varepsilon^2}\,z_{12} \;\sim\; \frac{2q_1}{p(\varepsilon)}, \tag{15}$$

$$k_2 \;=\; \frac{1}{\varepsilon^2}\,z_{22} \;\sim\; \frac{2q_1\,\varepsilon}{p(\varepsilon)\,\sqrt{q_2}}. \tag{16}$$

The closed-loop system matrix becomes

$$A_{cl} = \begin{pmatrix} 0 & 1 \\ -k_1 & -k_2 \end{pmatrix}, \tag{17}$$

which gives a characteristic equation of

$$\lambda^2 + k_2 \lambda + k_1 = 0.$$

If we denote the eigenvalues by λ_1 and λ_2, and write

$$(\lambda - \lambda_1)(\lambda - \lambda_2) = \lambda^2 - (\lambda_1 + \lambda_2)\lambda + \lambda_1 \lambda_2$$

as the characteristic equation, then we can solve for k_1 and k_2 as

$$\begin{aligned} k_1 &= \lambda_1 \lambda_2, \\ k_2 &= -(\lambda_1 + \lambda_2). \end{aligned}$$

Without loss of generality, assume $|\lambda_1| > |\lambda_2|$. As ε approaches zero, $-k_2$ follows the behavior of λ_1, and the ratio $-\frac{k_1}{k_2}$ follows the behavior of λ_2. Then with the current parameter choices and the expressions (15) and (16) we can see

$$\lambda_1 \sim -\frac{2q_1 \varepsilon}{p(\varepsilon)\sqrt{q_2}}, \tag{18}$$

$$\lambda_2 \sim -\frac{\sqrt{q_2}}{\varepsilon}. \tag{19}$$

We can also calculate the behavior of the parameter n from (2) and by taking the logarithm of (15) and (16)

$$n \sim \lim_{\varepsilon \to 0} \frac{\log_\varepsilon k_1}{\log_\varepsilon k_2} = \lim_{\varepsilon \to 0} \frac{\log_\varepsilon 2q_1 - c}{\log_\varepsilon 2q_1 + 1 - \log_\varepsilon \sqrt{q_2} - c} = \frac{c}{c-1}. \tag{20}$$

Note that in Case 1, both feedback gains approach infinity as ε approaches zero (γ approaches γ^*), since $p(\varepsilon) \ll \varepsilon^2$. Consequently, both eigenvalues approach negative infinity. Also note that for constant ε, we can let γ approach γ^* from above by increasing c. With this approach, the feedback gains and eigenvalues again approach positive and negative infinity, respectively, since $p(\varepsilon)$ is in the denominator of the gains and $p(\varepsilon) = \varepsilon^c$ goes to zero as c approaches infinity for small values of ε.

For each variation of the q_2 parameter presented below, the resulting controller gains approach infinity as γ approaches γ^*. The gains become large because the denominator of z_{12} goes to zero, as described above, or because the cost on the control, $R = \varepsilon^2$, becomes small and allows large control signals. We have tailored the H^∞ problem in this way to ensure we achieve the high-gain control that could cause the stability region to vanish. Section 3 will derive the conditions that prevent the stability region from vanishing, even with high-gain control.

We performed analyses similar to the one above for five other cases of different parameter classes as outlined in Appendix B. The different cases and the results of the analyses are summarized in Table 1. Since we are examining the rates at which the values change, the results in Table 1 contain only the relevant parameters and we have dropped any constant multipliers from the eigenvalue expressions for simplicity. In addition, we have written $p(\varepsilon)$ where appropriate, so that γ approaches γ^* as ε approaches zero if $c > 0$. In each case we can verify that the Z matrix is positive definite using conditions (15) and (16), and that $\bar{\gamma} = \gamma^*$.

The results in Table 1 indicate that each case allows some freedom in the selection of the parameter n. Cases 4 and 5 allow for the most complete selection of eigenvalue behavior because we can access both eigenvalues through the choices of l and c. All of the six cases allow for total freedom in the choice of the *relative* eigenvalue behavior, which can be defined as the parameter m in the equation $\lambda_1 = \lambda_2^m$. By adjusting the parameters q_2 and $p(\varepsilon)$ we have succeeded in using the H^∞ approach to adjust the behavior of the linear feedback gains and the closed-loop eigenvalues to suit our performance requirements.

Table 1: Behavior of n, λ_1 and λ_2 for the six parameter cases analyzed.

Case	q_2	$p(\varepsilon)$	c	n	$-\lambda_1$	$-\lambda_2$
1	$q_2 > 0$	$p(\varepsilon) = \varepsilon^c$	$c > 2$	$\frac{c}{c-1}$	$\frac{\varepsilon}{p(\varepsilon)}$	$\frac{1}{\varepsilon}$
2	$q_2 > 0$	$p(\varepsilon) = \varepsilon^c$	$c < 2$	$1 + \frac{c}{2}$	$\frac{1}{\varepsilon}$	$\frac{1}{\sqrt{p(\varepsilon)}}$
3	$q_2 = 0$	$p(\varepsilon) = \varepsilon^{1+c}$	$c > 0$	$\frac{2c+2}{2c+1}$	$\frac{\sqrt{\varepsilon}}{p(\varepsilon)}$	$\frac{1}{\sqrt{\varepsilon}}$
4	$q_2 = \varepsilon^l$, $0 < l < 1$	$p(\varepsilon) = \varepsilon^{l+c}$	$c > 2 - 2l$	$\frac{2(l+c)}{3l+2c-2}$	$\frac{\varepsilon^{(1-\frac{1}{2}l)}}{p(\varepsilon)}$	$\frac{1}{\varepsilon^{(1-\frac{1}{2}l)}}$
5	$q_2 = \varepsilon^l$, $0 < l < 1$	$p(\varepsilon) = \varepsilon^{l+c}$	$c < 2 - 2l$	$\frac{c+2}{2-l}$	$\frac{1}{\varepsilon^{(1-\frac{1}{2}l)}}$	$\frac{1}{\sqrt{p(\varepsilon)}}$
6	$q_2 = \varepsilon^l$, $1 \leq l$	$p(\varepsilon) = \varepsilon^{1+c}$	$c > 0$	$\frac{2c+2}{2c+1}$	$\frac{\sqrt{\varepsilon}}{p(\varepsilon)}$	$\frac{1}{\sqrt{\varepsilon}}$

The above results also indicate that the closed-loop system will exhibit a two time-scale behavior because the eigenvalues approach infinity at significantly different rates. A two time-scale behavior means that one of the state variables will converge much faster than the other. We can expect the slow variable to remain nearly constant while the fast variable converges. Then, the fast variable should remain relatively steady over the period of time required for the slow variable to converge. We will look for this type of behavior when we examine the results of our simulations.

Having stated and solved the problem of finding stabilizing gains for a second-order system, we now focus on maintaining the stability region. In the next section we develop a sufficient condition on the parameter n to ensure that the closed-loop system exhibits a nonvanishing stability region for a given maximum degree of the disturbance. We will translate this condition into a condition on c, the exponent parameter of $p(\varepsilon)$, for the cases we have already considered. Our analysis will show that each case allows for a range of parameter selections that ensure the stability region will not vanish as the gains increase.

3 Stability Analysis

We know that all of the controllers produced by the H^∞ techniques used in the previous section will yield closed-loop systems that are bounded-input bound-output stable [7]. Another important measure of stability, though, is the size of the stability region or the region of initial conditions that allow the system to reach a stable equilibrium point. As mentioned above, as we approach the optimal attenuation levels, we employ high-gain controllers so we want to understand what happens to the stability region as the gains increase. If the region shrinks, as described in [8] for some nonlinear disturbances, then the desired gains may result in a region of stability that is too small to be practical.

Our stability analysis is based on standard Lyapunov techniques to develop sufficient conditions on n in (2) such that the resulting closed-loop second-order system has a nonvanishing stability region as the gains increase. We will combine the result with our previous analysis to develop conditions on the design parameters $p(\varepsilon)$ and q_2 used in Section 2.

To develop the nonvanishing stability region, we will use the closed-loop system derived in Section 2 with minor changes to variables to simplify the analysis. Consider the closed-loop system without disturbances

$$\dot{x} = A_{cl}x \tag{21}$$

with

$$A_{cl} = \begin{pmatrix} 0 & 1 \\ -k^n & -k \end{pmatrix},$$

which is identical to A_{cl} in (17) if we let $k^n = k_1$, $k = k_2$, (or equivalently $u = -k^n x_1 - k x_2$ and no disturbances). Note that the parameter n is the same as in (2), and we will assume that $1 < n < 2$, since this is the complete range of n produced by the methods in the previous section in each of the six cases.

For the above choices of B and D, the algebraic Riccati equation (6) reduces to the Lyapunov equation

$$A_{cl}^T Z + Z A_{cl} + Q \;=\; 0. \tag{22}$$

We will choose a Q matrix that has a different form than the one we used in Section 2 because it allows us to more easily solve the problem. The new Q matrix, denoted $\tilde{Q}$, has ones for the off-diagonal terms. With this new matrix our analysis is still mathematically valid because we are using it to find a *bound* on the parameter n. In this case, the method we use to find the bound is not as important as the results. Now, with some foresight[2], set

$$Q \;=\; \tilde{Q} \;=\; \begin{pmatrix} k^{n-1} + q\,k^{2n-3} & 1 \\ 1 & k^{1-n} + p\,k^{-1} \end{pmatrix}, \qquad p \;>\; 0, \qquad q \;>\; 0, \tag{23}$$

and solve for Z from (22) to find

$$Z \;=\; \begin{pmatrix} \frac{1}{2}[(p+q+1)\,k^{n-2} + q\,k^{2n-4}] & \frac{1}{2}[k^{-1} + q\,k^{n-3}] \\ \frac{1}{2}[k^{-1} + q\,k^{n-3}] & \frac{1}{2}[k^{-n} + (p+1)\,k^{-2} + q\,k^{n-4}] \end{pmatrix}. \tag{24}$$

We take $V = x^T Z x$, as a Lyapunov function which is equivalent to

$$\begin{aligned} V(x_1,\,x_2) \;&=\; \frac{1}{2}\left\{\left[(p+q+1)\,k^{n-2} + q\,k^{2n-4}\right]\,x_1^2 + 2\left[k^{-1} + q\,k^{n-3}\right]x_1\,x_2\right. \\ &\quad \left. + \left[k^{-n} + (p+1)\,k^{-2} + q\,k^{n-4}\right]\,x_2^2\right\}. \end{aligned} \tag{25}$$

Theorem 1 *If the point $(x_1,\,x_2)$ is a part of the region defined by*

$$V(x_1,\,x_2) \;\leq\; M_1\,k^{n-2}, \tag{26}$$

where $M_1 > 0$ is a constant, and will continue to be a part of this region as k increases to infinity, then the following are true:

$$\begin{aligned} |x_1| \;&\leq\; O(1) \\ |x_2| \;&\leq\; O(k^{n-1}). \end{aligned}$$

Proof. We apply the Law of Cosines inequality $|2ab| \leq a^2 + b^2$ to the cross term in the expression for $V(x_1,\,x_2)$ to get

$$\begin{aligned} \left|2\left(\frac{1}{2}k^{-1} + \frac{1}{2}q\,k^{n-3}\right)x_1\,x_2\right| \;&=\; \left|2\left[\frac{1}{2}k^{-\frac{n}{2}}\,x_2\right]\left[(k^{\frac{n}{2}-1} + q\,k^{\frac{3n}{2}-3})x_1\right]\right| \\ &\leq\; \frac{1}{4}\,k^{-n}\,x_2^2 + \left[k^{\frac{1}{2}(n-2)} + qk^{\frac{3}{2}(n-2)}\right]^2 x_1^2. \end{aligned} \tag{27}$$

Now subtract the right hand side of (27) from V to get the following lower bound on V

$$\begin{aligned} V \;\geq\; &\left[\frac{1}{2}(p+q+1)k^{n-2} + \frac{1}{2}qk^{2(n-2)} - k^{n-2} - 2qk^{2(n-2)} - q^2\,k^{3(n-2)}\right]x_1^2 \\ &+ \left[\frac{1}{4}k^{-n} + \frac{1}{2}(p+1)k^{-2} + \frac{1}{2}qk^{n-4}\right]x_2^2. \end{aligned} \tag{28}$$

[2]We picked this particular structure for $\tilde{Q}$ because it admits a straightforward solution for Z with all entries depending on k. The exponents for the k terms were set to allow us to find a nonvanishing stability region.

Recall that $1 < n < 2$, which implies $n - 2 < 0$. For the expression (28), as k grows large, the term in which k has the largest exponent dominates the expression and the right hand side approaches

$$\frac{1}{2}(p+q-1)\,k^{n-2}\,x_1^2 + \frac{1}{4}k^{-n}\,x_2^2. \tag{29}$$

Now suppose that we can choose p and q such that $p+q > 1$, to keep expression (29) positive. For $(x_1,\, x_2)$ that continue to satisfy (26) as k grows large, we know the following inequalities hold:

$$\begin{aligned} M_1\,k^{n-2} &\geq \frac{1}{2}(p+q-1)k^{n-2}\,x_1^2 \\ M_1\,k^{n-2} &\geq \frac{1}{4}k^{-n}\,x_2^2. \end{aligned}$$

Then, to prevent the right hand sides of the above two expressions from growing faster than the left hand sides, the following must be true:

$$\begin{aligned} |x_1| &\leq O(1) \\ |x_2| &\leq O(k^{n-1}). \end{aligned}$$

□

Now we will activate the disturbance in the system and study the stability region in the presence of bounded perturbations. Consider the system (21), with A_{cl} the same as before and add Dw to the right-hand side with

$$D = \begin{pmatrix} 1 & 0 \\ 0 & 1 \end{pmatrix}, \quad w = \begin{pmatrix} w_1(x_1,\, x_2) \\ w_2(x_1,\, x_2) \end{pmatrix}$$

such that the following inequalities hold:

$$|w_1(x_1,\, x_2)| \leq M\,|x_1|^{\mu} \tag{30}$$

$$|w_2(x_1,\, x_2)| \leq M\,|x_1|^{\mu} + M\,|x_2|^{\nu}, \tag{31}$$

with $M > 0$, $\mu > 0$ and $\nu > 0$. These inequalities represent sector bounds on the possibly nonlinear disturbance terms. We can now state and prove the main results of this section.

Theorem 2 *Consider the following values of n for fixed ν:*

$$\begin{aligned} n &\in (1,2) \qquad \text{for } \nu \leq 2 \\ n &< 1 + \frac{1}{2\nu - 3} \qquad \text{for } \nu > 2 \end{aligned}$$

Then, $\dot{V} < 0$ on state trajectories within the region defined by (26), and the closed-loop system is asymptotically stable over the same region.

Before we begin the proof, we offer an explanatory note and an outline. The proof is lengthy and based on a single lemma which proves a key inequality. To prove $\dot{V} < 0$, we will expand the expression for $\dot{V}$ and then use the lemma (proved below) to find a bound on the positive portion of the expression. We construct the bound piece-by-piece such that the magnitude of the positive portion will be smaller than the magnitude of the negative portion of the expression. We will choose two fractional multipliers, $\frac{1}{8}$ and $\frac{1}{7}$, so that when we combine the various pieces, the positive portion is sufficiently small. We finally note that the argument holds only in the limit as the feedback gain k grows large.

Proof. We differentiate V on a state trajectory and, after some algebraic manipulation, we get

$$\begin{aligned}
\dot{V} &= -k^{n-1}\,(x_1 + k^{1-n}\,x_2)^2 - qk^{2n-3}\,x_1^2 - pk^{-1}\,x_2^2 + (k^{-1} + qk^{n-3})\,x_1\,w_2 \\
&\quad + \left[k^{-n} + (p+1)k^{-2} + qk^{n-4}\right]\,x_2\,w_2 + \left[(p+q+1)k^{n-2} + qk^{2n-4}\right]\,x_1\,w_1 \\
&\quad + (k^{-1} + qk^{n-3})\,x_2\,w_1 \\
&= -k^{n-1}\,(x_1 + k^{1-n}\,x_2)^2 - qk^{2n-3}\,x_1^2 - pk^{-1}\,x_2^2 + k^{-1}\,w_2\,(x_1 + k^{1-n}\,x_2) \\
&\quad + qk^{n-3}\,x_1\,w_2 + \left[(p+1)k^{-2} + qk^{n-4}\right]\,x_2\,w_2 + k^{n-2}\,w_1(x_1 + k^{1-n}\,x_2) \\
&\quad + \left[(p+q)k^{n-2} + qk^{2n-4}\right]\,x_1\,w_1 + qk^{n-3}\,x_2\,w_1 \\
&= -k^{n-1}\,(x_1 + k^{1-n}\,x_2)^2 - qk^{2n-3}\,x_1^2 - pk^{-1}\,x_2^2 \\
&\quad + k^{n-2}(w_1 + k^{1-n}\,w_2)(x_1 + k^{1-n}\,x_2) + \left[(p+q)k^{n-2} + qk^{2n-4}\right]\,x_1\,w_1 \\
&\quad + qk^{n-3}\,x_2\,w_1 + qk^{n-3}\,x_1\,w_2 + \left[(p+1)k^{-2} + qk^{n-4}\right]\,x_2\,w_2
\end{aligned} \tag{32}$$

As an intermediate step, we now prove the following lemma:

Lemma 1 *As k approaches infinity,*

$$\left\{\begin{array}{l} k^{n-2}\,(w_1 + k^{1-n}\,w_2)(x_1 + k^{1-n}\,x_2) \\ + \left[(p+q)k^{n-2} + qk^{2n-4}\right]\,x_1\,w_1 \\ + qk^{n-3}\,x_2\,w_1 + qk^{n-3}\,x_1\,w_2 \\ + \left[(p+1)k^{-2} + q\,k^{n-4}\right]\,x_2\,w_2 \end{array}\right\} \leq \left\{\begin{array}{l} \frac{1}{2}k^{n-1}(x_1 + k^{1-n}\,x_2)^2 + \frac{7}{8}\,qk^{2n-3}\,x_1^2 \\ + \frac{6}{7}\,pk^{-1}\,x_2^2 \end{array}\right\} \tag{33}$$

provided that $n < 1 + \frac{1}{2\nu-3}$ for $\nu > 2$.

Proof. We will find a bound for each term on the left hand side of (33) and then combine the results to prove the lemma. Applying the Law of Cosines inequality to the first term on the left hand side of (33), we find that

$$k^{n-2}\,(w_1 + k^{1-n}\,w_2)(x_1 + k^{1-n}\,x_2) \;\leq\; \frac{1}{2}\left[k^{n-1}\,(x_1 + k^{1-n}\,x_2)^2 + k^{n-3}\,(w_1 + k^{1-n}\,w_2)^2\right],$$

or

$$\begin{aligned}
&k^{n-2}\,(w_1 + k^{1-n}\,w_2)(x_1 + k^{1-n}\,x_2) \;\leq \\
&\qquad \frac{1}{2}\,k^{n-1}\,(x_1 + k^{1-n}\,x_2)^2 + \frac{1}{2}\,k^{n-3}\,w_1^2 + k^{-2}\,w_1\,w_2 + \frac{1}{2}\,k^{-1-n}\,w_2^2.
\end{aligned} \tag{34}$$

The first term on the right hand side of (34) is in an acceptable form for our analysis, so we will leave it alone. Taking the second term on the right hand side of (34), if

$$\frac{1}{2}\,k^{n-3}\,M^2\,|x_1|^{2\mu} \;\leq\; \frac{q}{8}\,k^{2n-3}\,x_1^2,$$

then

$$\frac{k^{n-3}}{2}\,w_1^2 \;\leq\; \frac{q}{8}\,k^{2n-3}\,x_1^2.$$

Both of these inequalities are true as k approaches infinity, since $2n-3 > n-3$. Now take the third term of the right hand side of (34) and use the sector bounds on the disturbances, to get:

$$|k^{-2}\, w_1\, w_2| \;\leq\; \left|\left[k^{-2}\, M^2\, |x_1|^{\mu}\, |x_2|^{\nu}\right]\right| + \left|\left[k^{-2}\, M^2\, |x_1|^{2\mu}\right]\right|,$$

and so

$$|k^{-2}\, w_1\, w_2| \;\leq\; \frac{1}{2}\, k^{2n-3-\epsilon}\, M^2\, |x_1|^{2\mu} + \frac{1}{2}\, k^{-1-2n+\epsilon}\, M^2\, |x_2|^{2\nu} + k^{-2}\, M^2\, |x_1|^{2\mu}, \tag{35}$$

for some small $\epsilon > 0$. The first and third terms of the right hand side of (35) can be grouped to show that

$$(\frac{1}{2}\, k^{2n-3-\epsilon} + k^{-2})\, M^2\, |x_1|^{2\mu} \;\leq\; \frac{q}{8}\, k^{2n-3}\, x_1^2,$$

as k approaches infinity, since $2n-3-\epsilon < 2n-3$ and $-2 < 2n-3$. The second term of (35) can be treated as follows:

$$\frac{1}{2}\, k^{-1-2n+\epsilon}\, M^2\, |x_2|^{2\nu} \;\leq\; \frac{p}{7}\, k^{-1}\, x_2^2,$$

which is equivalent to saying

$$|x_2|^{2\nu-2} \;\leq\; \frac{2p}{7M^2}\, k^{2n-\epsilon},$$

and by applying Theorem 1, these two inequalities will be true as k approaches infinity if $2(\nu-1)(n-1) \leq 2n-\epsilon$. Since we can choose ϵ arbitrarily small, this condition is equivalent to

$$n \;<\; 1 + \frac{1}{\nu-2}, \qquad \text{for } \nu \;>\; 2, \tag{36}$$

and for $\nu \leq 2$ it will always be satisfied. We have shown, then, that when (36) is satisfied, and for k approaching infinity,

$$|k^{-2}\, w_1\, w_2| \;\leq\; \frac{q}{8}\, k^{2n-3}\, x_1^2 + \frac{p}{7}\, k^{-1}\, x_2^2. \tag{37}$$

Now we can bound the fourth term on the right hand side of (34) as follows:

$$\begin{aligned}
\frac{1}{2}\, k^{-1-n}\, w_2^2 \;&\leq\; \frac{1}{2}\, k^{-1-n}\, M^2\, (|x_1|^{\mu} + |x_2|^{\nu})^2 \\
&=\; \frac{1}{2}\, k^{-1-n}\, M^2\, x_1^{2\mu} + k^{-1-n}\, M^2\, |x_1|^{\mu}\, |x_2|^{\nu} + \frac{1}{2}\, k^{-1-n}\, M^2\, x_2^{2\nu} \\
&\leq\; k^{-1-n}\, M^2\, x_1^{2\mu} + k^{-1-n}\, M^2\, x_2^{2\nu},
\end{aligned} \tag{38}$$

where in the last inequality, we again used the Law of Cosines relationship. We know that, for large k,

$$k^{-1-n}\, M^2\, x_1^{2\mu} \;\leq\; \frac{q}{8}\, k^{2n-3}\, x_1^2,$$

since $2n-3 > -1-n$. Also, if we restrict n such that

$$n \;>\; 2(\nu-1)(n-1) \tag{39}$$

we can show

$$k^{-1-n}\, M^2\, x_2^{2\nu} \;\leq\; \frac{p}{7}\, k^{-1}\, x_2^2,$$

or equivalently

$$x_2^{2(\nu-1)} \;\leq\; \frac{p}{7M^2}\, k^n$$

as k approaches infinity. The condition on n in (39) is equivalent to

$$n \;<\; 1 + \frac{1}{2\nu - 3}, \qquad \text{for } \nu \;>\; \frac{3}{2}, \tag{40}$$

and it will always be satisfied for $\nu < \frac{3}{2}$. We have thus shown that if (40) holds, then

$$\frac{1}{2}\, k^{-1-n}\, w_2^2 \;\leq\; \frac{q}{8}\, k^{2n-3}\, x_1^2 + \frac{p}{7}\, k^{-1}\, x_2^2. \tag{41}$$

Now, combining the results from the arguments since (34), we have

$$k^{n-2}\,(w_1 + k^{1-n}\, w_2)(x_1 + k^{1-n}\, x_2) \;\leq\; \frac{1}{2}\, k^{n-1}\,(x_1 + k^{1-n}\, x_2)^2 + \frac{3q}{8}\, k^{2n-3}\, x_1^2 + \frac{2p}{7}\, k^{-1}\, x_2^2. \tag{42}$$

The expression in (42) is a convenient bound on the first term in (33). We will next find similar bounds for the remaining terms on the left hand side of (33). For the second term, we find that

$$\left|\left[(p+q)k^{n-2} + qk^{2n-4}\right]\, x_1\, w_1\right| \;\leq\; \frac{q}{8}\, k^{2n-3}\, x_1^2, \tag{43}$$

since $2n - 3 > n - 2$ and $2n - 3 > 2n - 4$, which takes care of the second term. The third term on the left hand side of (33) can be bound as

$$qk^{n-3}\,|x_2\, w_1| \;\leq\; \frac{q}{2}\,(k^{2n-3-\epsilon}\, w_1^2 + k^{-3+\epsilon}\, x_2^2) \tag{44}$$

for some small $\epsilon > 0$. Applying the Law of Cosines inequality again, we see

$$\frac{q}{2}\, k^{2n-3-\epsilon}\, w_1^2 \;\leq\; \frac{q}{2}\, k^{2n-3-\epsilon}\, M^2\, |x_1|^{2\mu} \;\leq\; \frac{q}{8}\, k^{2n-3}\, x_1^2 \tag{45}$$

as k approaches infinity. Similarly, if $\epsilon < 2$, then

$$\frac{q}{2}\, k^{-3+\epsilon}\, x_2^2 \;\leq\; \frac{p}{7}\, k^{-1}\, x_2^2. \tag{46}$$

From the inequalities (44), (45) and (46), then we have that as k approaches infinity, the inequality

$$qk^{n-3}\,|x_2\, w_1| \;\leq\; \frac{q}{8}\, k^{2n-3}\, x_1^2 + \frac{p}{7}\, k^{-1}\, x_2^2 \tag{47}$$

holds. Now taking the fourth term on the left hand side of (33) we can show

$$\begin{aligned} |qk^{n-3}\, x_1\, w_2| \;&\leq\; qk^{n-3}\, M\,\left(|x_1|^{\mu+1} + |x_1||x_2|^{\nu}\right) \\ &\leq\; qk^{n-3}\, M|x_1|^{\mu+1} + \frac{q}{2}\, M\,\left(k^{2n-3-\epsilon}\, x_1^2 + k^{-3+\epsilon}\,|x_2|^{2\nu}\right) \end{aligned}$$

for some small $\epsilon > 0$. We then have that as k approaches infinity,

$$qk^{n-3}\, M\,|x_1|^{\mu+1} + \frac{q}{2}\, M\, k^{2n-3-\epsilon}\, x_1^2 \;\leq\; \frac{q}{8}\, k^{2n-3}\, x_1^2. \tag{48}$$

We can also say that as k approaches infinity,

$$\frac{q}{2}\, M\, k^{-3+\epsilon}\,|x_2|^{2\nu} \;\leq\; \frac{p}{7}\, k^{-1}\, x_2^2,$$

which is equivalent to saying

$$|x_2|^{2(\nu-1)} \;\leq\; \frac{2p}{7qM}\, k^{2-\epsilon},$$

provided that $2(\nu-1)(n-1) < 2-\epsilon$. Since we can choose ϵ arbitrarily small, this condition becomes

$$n \;<\; 1+\frac{1}{\nu-1}, \qquad \text{for } \nu > 1, \tag{49}$$

and it will always be satisfied for $\nu \leq 1$. If (49) is satisfied, then we have shown that as k approaches infinity,

$$|qk^{n-3}\, x_1\, w_2| \;\leq\; \frac{q}{8}\, k^{2n-3}\, x_1^2 + \frac{p}{7}\, k^{-1}\, x_2^2. \tag{50}$$

Now for the fifth and final term on the left hand side of (33), we use the fact that $1 < n < 2$ to show the following inequalities

$$\begin{aligned}
\left|\left[(p+1)k^{-2} + q\,k^{n-4}\right]\, x_2\, w_2\right| \;&\leq\; |(p+q+1)k^{-2}\, x_2\, w_2| \\
&\leq\; (p+q+1)M\, k^{-2}\, \left(|x_2|^{\nu+1} + |x_2||x_1|^{\mu}\right) \\
&\leq\; (p+q+1)M\, k^{-2}\, |x_2|^{\nu+1} \\
&\quad + \frac{1}{2}\,(p+q+1)M\, \left(k^{2n-3-\epsilon}\, |x_1|^{2\mu} + k^{-1-2n+\epsilon}\, |x_2|^2\right).
\end{aligned}$$

As before, we let k approach infinity to get

$$(p+q+1)M\, k^{-2}\, |x_2|^{\nu+1} \;\leq\; \frac{p}{7}\, k^{-1}\, x_2^2,$$

if $n < 1 + \frac{1}{\nu-1}$ for $\nu > 1$. We can also say that

$$\frac{1}{2}\,(p+q+1)M\, k^{2n-3-\epsilon}\, |x_1|^{2\mu} \;\leq\; \frac{q}{8}\, k^{2n-3}\, x_1^2,$$

and that

$$\frac{1}{2}\,(p+q+1)M\, k^{-1-2n+\epsilon}\, |x_2|^2 \;\leq\; \frac{p}{7}\, k^{-1}\, x_2^2,$$

provided ϵ is sufficiently small and k is sufficiently large. We have thus shown that if (49) is satisfied,

$$\left|\left[(p+1)k^{-2} + q\,k^{n-4}\right]\, x_2\, w_2\right| \;\leq\; \frac{q}{8}\, k^{2n-3}\, x_1^2 + \frac{2p}{7}\, k^{-1}\, x_2^2. \tag{51}$$

Lemma 1 follows from (42), (43), (47), (50) and (51), given the following conditions on the parameter n:

$$\begin{aligned}
n \;&<\; 1+\frac{1}{\nu-2}, && \nu \;>\; 2 \\
n \;&<\; 1+\frac{1}{2\nu-3}, && \nu \;>\; \frac{3}{2} \\
n \;&<\; 1+\frac{1}{\nu-1}, && \nu \;>\; 1.
\end{aligned}$$

The third condition subsumes the first condition, so we can ignore the latter. We are only considering n such that $1 < n < 2$, so the second and third conditions are not binding for $\nu \leq 2$. For $\nu > 2$, the second condition subsumes the third, so the second condition is the only one we need to enforce. Therefore, the final form of the condition on n is

$$n \;<\; 1+\frac{1}{2\nu-3}, \qquad \nu > 2, \tag{52}$$

which completes the proof of the lemma. □

It follows directly from the results of Lemma 1 that

$$\dot{V} \leq -\frac{1}{2}\,k^{n-1}\,(x_1 + k^{1-n}\,x_2)^2 - \frac{q}{8}\,k^{2n-3}\,x_1^2 - \frac{p}{7}\,k^{-1}\,x_2^2 \;<\; 0,$$

in the region defined by (26), which completes the proof of Theorem 2. □

Theorem 2 states that the stability region for the system must contain the region defined by (26). With this theorem in hand, we can now prove that the stability regions do not vanish as the feedback gains increase.

Theorem 3 *The region defined by (26) is a nonvanishing one as k approaches infinity.*

Proof. Using (25) and (27), we can show

$$V(x_1,\,x_2) \;\leq\; \left\{ \begin{array}{l} \frac{1}{2}\left[(p+q+1)k^{n-2} + qk^{2(n-2)} + 2\left(k^{\frac{1}{2}(n-2)} + qk^{\frac{3}{2}(n-2)}\right)^2\right] x_1^2 \\ +\,\frac{1}{2}\left[k^{-n} + (p+1)k^{-2} + qk^{n-4} + \frac{1}{2}\,k^{-n}\right] x_2^2 \end{array} \right\}.$$

We can then conclude that the region defined by

$$\left\{ \begin{array}{l} \frac{1}{2}\left[(p+q+3)k^{n-2} + 5qk^{2(n-2)} + 2q^2\,k^{3n-6}\right] x_1^2 \\ +\,\frac{1}{2}\left[\frac{3}{2}\,k^{-n} + (p+1)k^{-2} + qk^{n-4}\right] x_2^2 \end{array} \right\} \;\leq\; M_1\,k^{n-2} \tag{53}$$

is a subset of the region defined by (26). We can rewrite (53) as

$$\left\{ \begin{array}{l} \frac{1}{2}\left[(p+q+3) + 5qk^{n-2} + 2q^2\,k^{2n-4}\right] x_1^2 \\ +\,\frac{1}{2}\left[\frac{3}{2}k^{2-2n} + (p+1)k^{-n} + qk^{-2}\right] x_2^2 \end{array} \right\} \;\leq\; M_1, \tag{54}$$

which is a closed ellipse. The ellipse has one axis converging to a constant and the other expanding to infinity as k approaches infinity. The region defined by (26), therefore, must be nonvanishing as k approaches infinity. □

We can now state a theorem which summarizes the main results of this section.

Theorem 4 *The stability region for the closed-loop system described by (3), (30) and (31), and under linear feedback $u = -k^n x_1 - kx_2$, will be nonvanishing as the feedback gains approach infinity if (52) is satisfied.*

Proof. The theorem follows directly from the results of Theorems 2 and 3. □

We can translate condition (52) in terms of the parameters used in Section 2. For example, in Case 1 from Table 1, condition (52) becomes

$$\frac{c}{c-1} < 1 + \frac{1}{2\nu - 3}, \qquad \nu > 2,$$

which can be developed as follows, with $\nu > 2$ throughout:

$$c < \frac{(2\nu-2)(c-1)}{2\nu-3} \iff \left[1 - \left(\frac{2\nu-2}{2\nu-3}\right)\right] c < \frac{2-2\nu}{2\nu-3}$$

$$\iff \frac{-1}{2\nu-3}\,c < \frac{2-2\nu}{2\nu-3} \iff c > 2\nu - 2 \tag{55}$$

We performed a similar translation for the other five cases listed in Table 1 and Table 2 contains the resulting conditions. See Appendix C for details. We can conclude from our analysis that all six cases we have considered contain a range of parameter selection that will satisfy (52) and therefore guarantee a nonvanishing stability region. Note that in Case 4, the condition $c > 2\nu - 2$, $\nu > 2$ is sufficient for all values of l contained in the case. Also note that in Case 5, it is necessary that l is chosen so that $l < \frac{1}{\nu-1}$ for a valid $c > 0$ to exist.

Table 2: Stability conditions in terms of the design parameters. Note, in all cases $\nu > 2$.

Case	q_2	$p(\varepsilon)$	c	Condition on c
1	$q_2 > 0$	$p(\varepsilon) = \varepsilon^c$	$c > 2$	$c > 2\nu - 2$
2	$q_2 > 0$	$p(\varepsilon) = \varepsilon^c$	$c < 2$	$c < \frac{2}{2\nu-3}$
3	$q_2 = 0$	$p(\varepsilon) = \varepsilon^{1+c}$	$c > 0$	$c > \nu - 2$
4	$q_2 = \varepsilon^l$, $0 < l < 1$	$p(\varepsilon) = \varepsilon^{l+c}$	$c > 2 - 2l$	$c > \nu(2-l) - 2$
5	$q_2 = \varepsilon^l$, $0 < l < 1$	$p(\varepsilon) = \varepsilon^{l+c}$	$c < 2 - 2l$	$c < \frac{2+2\,l\,(1-\nu)}{2\nu-3}$
6	$q_2 = \varepsilon^l$, $1 \leq l$	$p(\varepsilon) = \varepsilon^{1+c}$	$c > 0$	$c > \nu - 2$

In applying these conditions in the structure of Section 2, it is important to note that the sector bound on the disturbance is often unknown. In this situation, we would complete our design using a guess for the value of ν and test the results. If we found the stability region vanished with increasing gain, we would increase the value of ν until we found an acceptable solution.

We have stated and solved the H^∞ control problem for a second order system and found a sufficient condition for the stability region to be nonvanishing as the feedback gains increase. To verify our analysis, we will next simulate a system and study the stability region as the gains are increased.

4 Simulation Results

As a test case we selected a second-order system with a nonlinear disturbance term similar to the first example in [8]. The system state equations are

$$\dot{x}_1 = x_2 \tag{56}$$

$$\dot{x}_2 = -k_1\, x_1 - k_2\, x_2 + x_2^3. \tag{57}$$

We selected this system because if we set $k_1 = k_2^2$ and allow the gains to increase to infinity, the stability region will vanish. This system can be expressed in the standard form

$$\dot{x} = Ax + Bu + Dw \tag{58}$$

with

$$A = \begin{pmatrix} 0 & 1 \\ 0 & 0 \end{pmatrix}, \quad B = \begin{pmatrix} 0 \\ 1 \end{pmatrix}, \quad D = \begin{pmatrix} 1 & 0 \\ 0 & 1 \end{pmatrix},$$

and control input

$$u = -R^{-1}B^T Z x$$

and disturbances

$$w = \begin{pmatrix} 0 \\ x_2^3 \end{pmatrix}.$$

Note that the disturbance term can be bounded by a sector bound of the form of (31), with $\nu = 3$, which allows us to directly apply the results from Section 3. To solve the algebraic Riccati equation we selected the following Q and R expressions:

$$Q = \begin{pmatrix} 1 & 0 \\ 0 & q_2 \end{pmatrix}, \qquad R = \varepsilon^2 > 0. \tag{59}$$

We note that the expression for Q here is consistent with our original definition in Section 2, but is different from that given in (23). Recall that we used (23) to find a condition on the parameter n to ensure a nonvanishing stability region. The choice of Q in (59) is part of the performance function for our disturbance attenuation measurement given in (4) and still provides a stable solution.

Using the system described above, we outline our simulation as follows:

1. Select a form for q_2 and $p(\varepsilon)$ which corresponds to one of the six cases presented in Section 2.
2. Use the sector bound parameter ν and the conditions in Table 2 to determine appropriate values for c and, if necessary, l.
3. Pick a small value for $\varepsilon > 0$.
4. Compute q_2 and $p(\varepsilon)$.
5. Compute γ^* using $\gamma^* = \frac{1}{\sqrt{2}} \left[q_2 + \varepsilon^2 + (q_2^2 - 2q_2\,\varepsilon^2 + \varepsilon^4 + 4q_1\,\varepsilon^2)^{\frac{1}{2}} \right]^{\frac{1}{2}}$.
6. Solve for Z using $A^T Z + ZA - Z(BR^{-1}B^T - \frac{1}{\gamma^2} DD^T)Z + Q = 0$.
7. Compute $A_{cl} = (A - BR^{-1}B^T Z)$.
8. Simulate the system in MATLAB using A_{cl} to estimate the stability region. For this step we give the system a small nonzero initial condition and let the system run in reverse time to find the stable limit cycle around the equilibrium point at the origin. See [2] for details on this trajectory reversing technique.
9. Adjust the value of ε and return to Step 4.

For our first simulation, we selected Case 5 from Table 1 with

$$q_2 = \varepsilon^l, \qquad l = \frac{1}{4}$$

$$p(\varepsilon) = \varepsilon^{l+c}, \qquad c = \frac{1}{4}.$$

For the disturbance given above with $\nu = 3$ and using the results in Table 2, we must choose $c < \frac{1}{3}$ to guarantee a nonvanishing stability region. For $c = \frac{1}{3}$, $l = \frac{1}{4}$ and the formula from Table 1 for n, we compute the maximum value for n as $\frac{4}{3}$. With $c = \frac{1}{4}$ the actual value of n is $\frac{9}{7}$, which is less than the maximum, so the stability region should not vanish. We note that the value of n is the important factor in determining how the stability region behaves. The specific choices for q_2 and $p(\varepsilon)$ are not critical.

We followed the procedure outlined above to simulate the system, and Figure 1 displays the graphical results. Table 3 contains the numerical values for the key parameters in the simulation as we vary ε. Figure 1(a) shows the estimated stability region for different values of ε. The stability region initially contracts and then expands along the x_1-axis while it continuously expands along the x_2-axis. The plots in Figure 1(b) show the maximum and minimum values for x_1 and x_2 versus ε on a semi-log scale to simplify the interpretation of the stability region estimates.

To explore the behavior of our system in a little more detail we included the results presented in Figures 2 and 3. In Figure 2(a) we plot the two eigenvalues obtained during the simulation against their predicted values. The top row in Figure 2(a) compares the eigenvalues to their values estimated using the formulas in Table 1. Since we dropped the constants in Table 1, we expect the line to be straight with a slope different

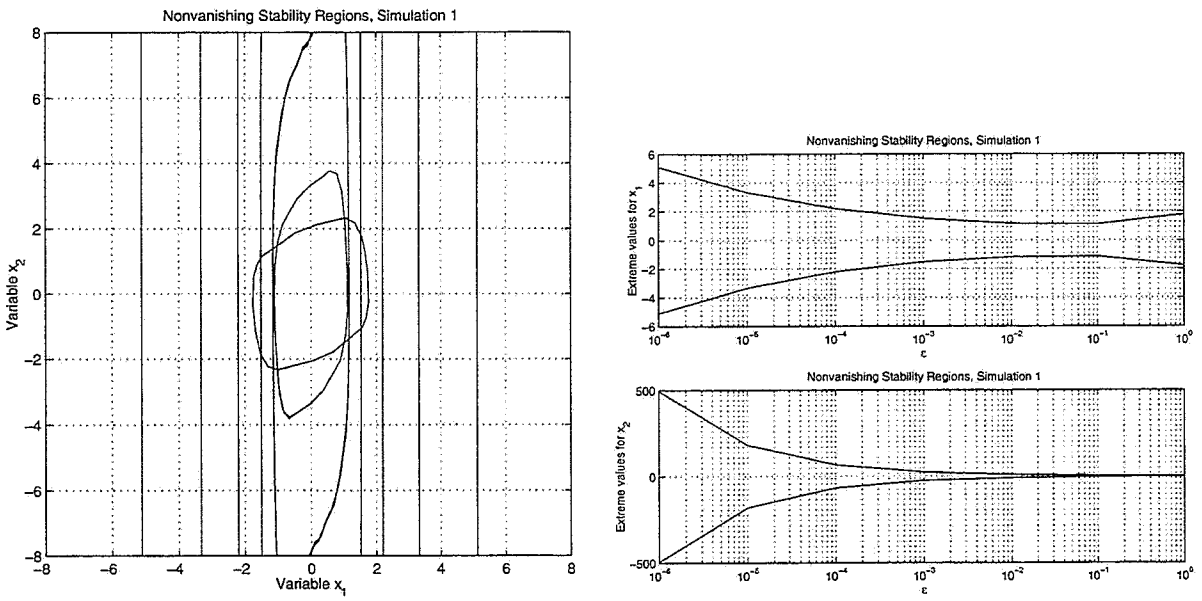

(a) (b)

Figure 1: Simulation 1. Case 5 with parameter values: $q_2 = \varepsilon^{\frac{1}{4}}$, $p(\varepsilon) = \varepsilon^{\frac{1}{2}}$, and $n = \frac{9}{7}$. Part (a) shows the simulated stability region boundary as the value of ε decreases. Part (b) plots the extreme values for state variables x_1 and x_2 versus ε.

Table 3: Simulation 1 numerical results. The table contains the absolute value of each quantity to simplify comparisons.

ε	$p(\varepsilon)$	γ^{*2}	k_1	k_2	λ_1	λ_2
1.00e+00	1.00e+00	2.00e+00	3.00e+00	3.87e+00	2.80e+00	1.07e+00
1.00e-01	3.16e-01	5.80e-01	2.02e+01	1.01e+01	7.38e+00	2.74e+00
1.00e-02	1.00e-01	3.17e-01	2.14e+02	6.00e+01	5.62e+01	3.81e+00
1.00e-03	3.16e-02	1.78e-01	2.61e+03	4.28e+02	4.22e+02	6.18e+00
1.00e-04	1.00e-02	1.00e-01	3.33e+04	3.17e+03	3.16e+03	1.05e+01
1.00e-05	3.16e-03	5.62e-02	4.34e+05	2.37e+04	2.37e+04	1.83e+01
1.00e-06	1.00e-03	3.16e-02	5.71e+06	1.78e+05	1.78e+05	3.21e+01

from one. The bottom row in Figure 2(a) compares the eigenvalues to the gain expressions we developed in Section 2. Again, we see the linear behavior we expected. Figure 2(b) confirms that the ratio $p(\varepsilon)/\gamma^{*2}$ approaches zero as ε goes to zero. Recall that we required this condition to ensure that γ approached γ^* as ε became small.

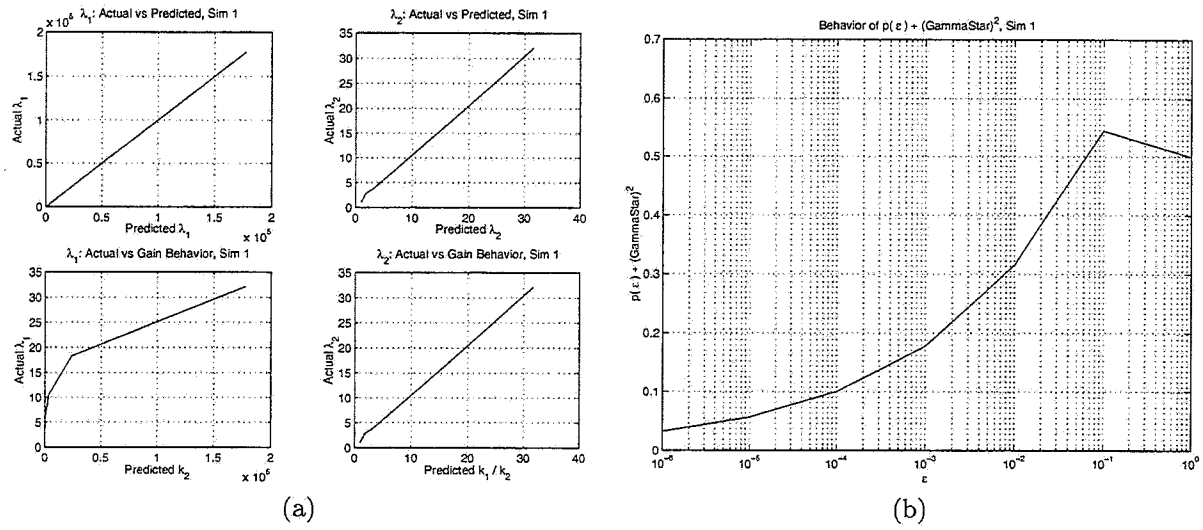

Figure 2: Simulation 1. Part (a) eigenvalue relationships as ε varies. Part (b) behavior of $p(\varepsilon)/\gamma^{*2}$ as $\varepsilon \to 0$.

Figure 3 captures the two time-scale behavior of the system for this simulation with $\varepsilon = 10^{-6}$. In Figure 3 the plots in the left column show each state variable plotted versus time. The two time-scale behavior becomes apparent when we stretch the time axis as shown in the right column of Figure 3. We can see that the variable x_1 is nearly constant during the time required for x_2 converge to a steady-state value. Then, the x_2 variable changes relatively slowly while x_1 transitions through its range of values. This cycle repeats because the state variables are traversing a stable limit cycle in this simulation. To clarify these results, we recall that we ran the simulation in reverse time, which explains why the trajectory starts at a small value and approaches a stable limit cycle. If we were to run the simulation in forward time, any initial condition within the limit cycle would converge to the stable equilibrium point at the origin.

For this simulation, the value for n satisfies the sufficient condition we established in Section 3 and the results confirm the stability region is expanding as the feedback gains increase. The next simulation highlights the fact that our condition on n is only sufficient and not necessary.

For our second simulation, we made the following parameter choices:

$$q_2 = \varepsilon^l, \qquad l = \frac{1}{4}$$

$$p(\varepsilon) = \varepsilon^{l+c}, \qquad c = \frac{1}{2}.$$

These choices correspond to Case 5 with $n = \frac{10}{7}$. Since the value for $\nu = 3$ has not changed, both c and n are now larger than the maximum values specified by our sufficient conditions. We simulated the system and found that the stability region did not vanish as the gains increased, as shown in Figure 4. As we saw in the first simulation, the stability region initially contracts and then expands along the x_1-axis, while it continuously expands along the x_2-axis. The expansion along the x_1-axis occurs at a smaller value for ε, which indicates we must increase the feedback gains to larger values for the stability region to expand. These results are a clear indication that the condition (52) does not provide a tight bound on the parameter n to achieve a nonvanishing stability region.

To allow for a complete comparison between the first and second simulations, we have included Table 4 and Figures 5 and 6, which correspond to the table and figures presented for the first simulation.

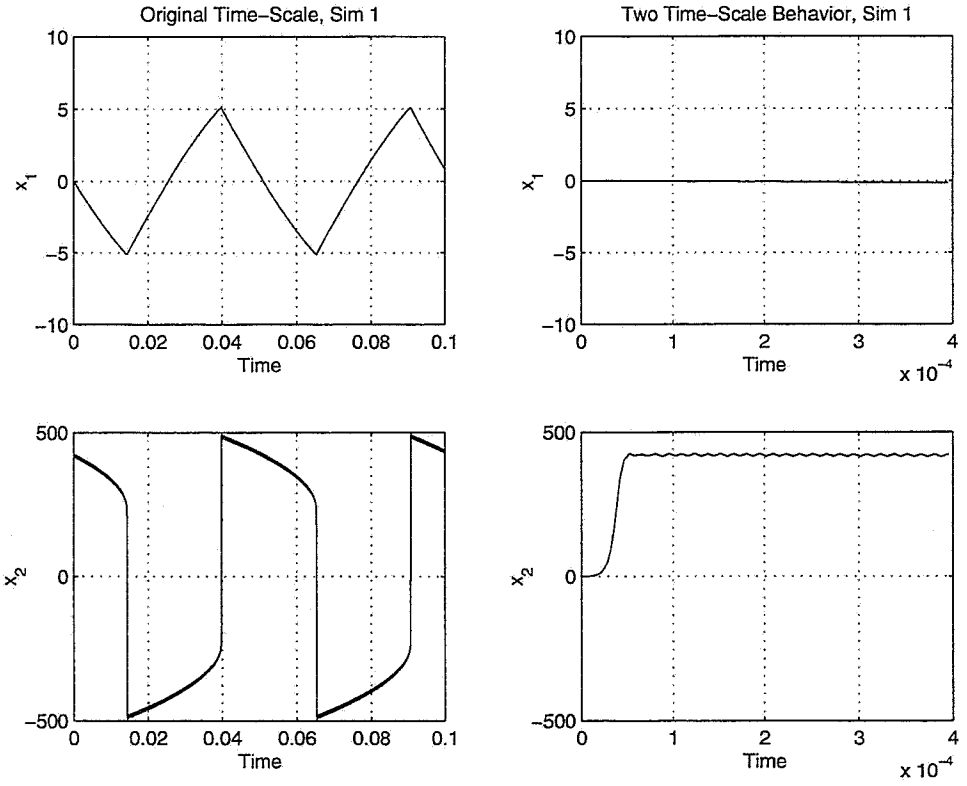

Figure 3: Simulation 1. Two time-scale behavior for $\varepsilon = 1.0 \times 10^{-6}$. Note the variable ranges differ by two orders of magnitude.

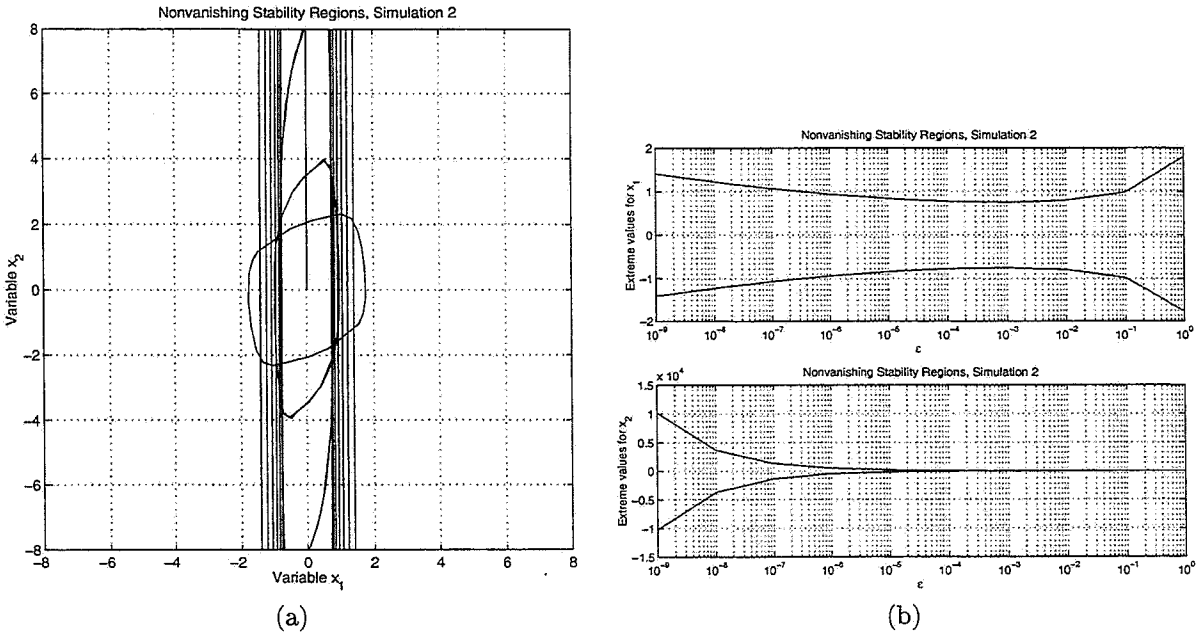

(a) (b)

Figure 4: Simulation 2. Parameter values: $q_2 = \varepsilon^{\frac{1}{4}}$, $p(\varepsilon) = \varepsilon^{\frac{3}{4}}$, and $n = \frac{10}{7}$. Part (a) shows the simulated stability region boundary as the value of ε decreases. Part (b) plots the extreme values for state variables x_1 and x_2 versus ε.

Table 4: Simulation 2 numerical results. The table contains the absolute value of each quantity to simplify comparisons.

ε	$p(\varepsilon)$	γ^{*2}	k_1	k_2	λ_1	λ_2
1.00e+00	1.00e+00	2.00e+00	3.00e+00	3.87e+00	2.80e+00	1.07e+00
1.00e-01	1.78e-01	5.80e-01	2.68e+01	1.10e+01	7.35e+00	3.65e+00
1.00e-02	3.16e-02	3.17e-01	3.65e+02	6.27e+01	5.62e+01	6.49e+00
1.00e-03	5.62e-03	1.78e-01	5.89e+03	4.36e+02	4.22e+02	1.40e+01
1.00e-04	1.00e-03	1.00e-01	1.02e+05	3.19e+03	3.16e+03	3.21e+01
1.00e-05	1.78e-04	5.62e-02	1.79e+06	2.38e+04	2.37e+04	7.53e+01
1.00e-06	3.16e-05	3.16e-02	3.17e+07	1.78e+05	1.78e+05	1.78e+02
1.00e-07	5.62e-06	1.78e-02	5.63e+08	1.33e+06	1.33e+06	4.22e+02
1.00e-08	1.00e-06	1.00e-02	1.00e+10	1.00e+07	1.00e+07	1.00e+03
1.00e-09	1.78e-07	5.62e-03	1.78e+11	7.50e+07	7.50e+07	2.37e+03

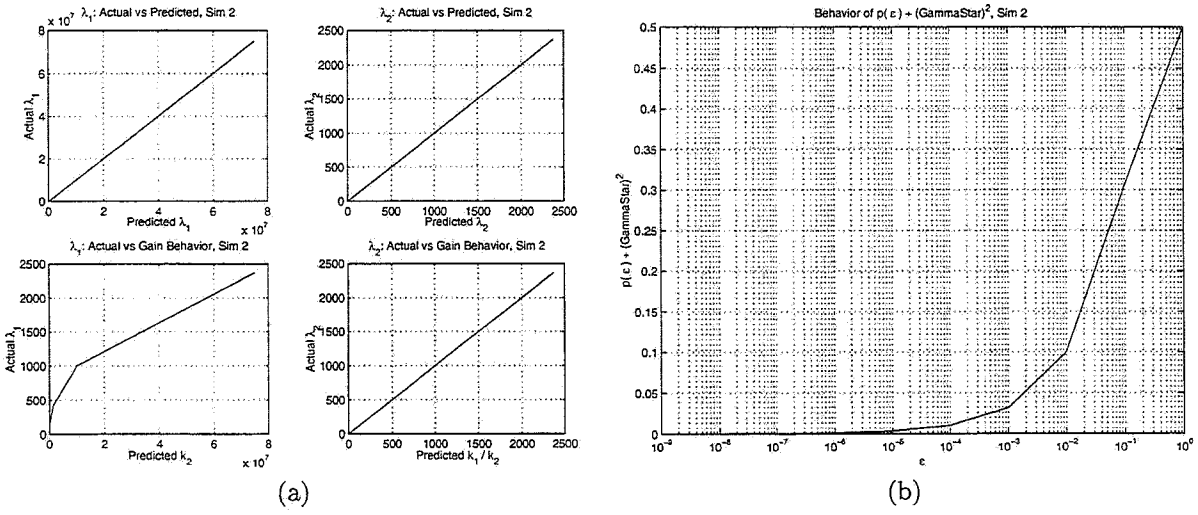

(a) (b)

Figure 5: Simulation 2. Part (a) eigenvalue relationships as ε varies. Part (b) behavior of $p(\varepsilon)/\gamma^{*2}$ as $\varepsilon \to 0$.

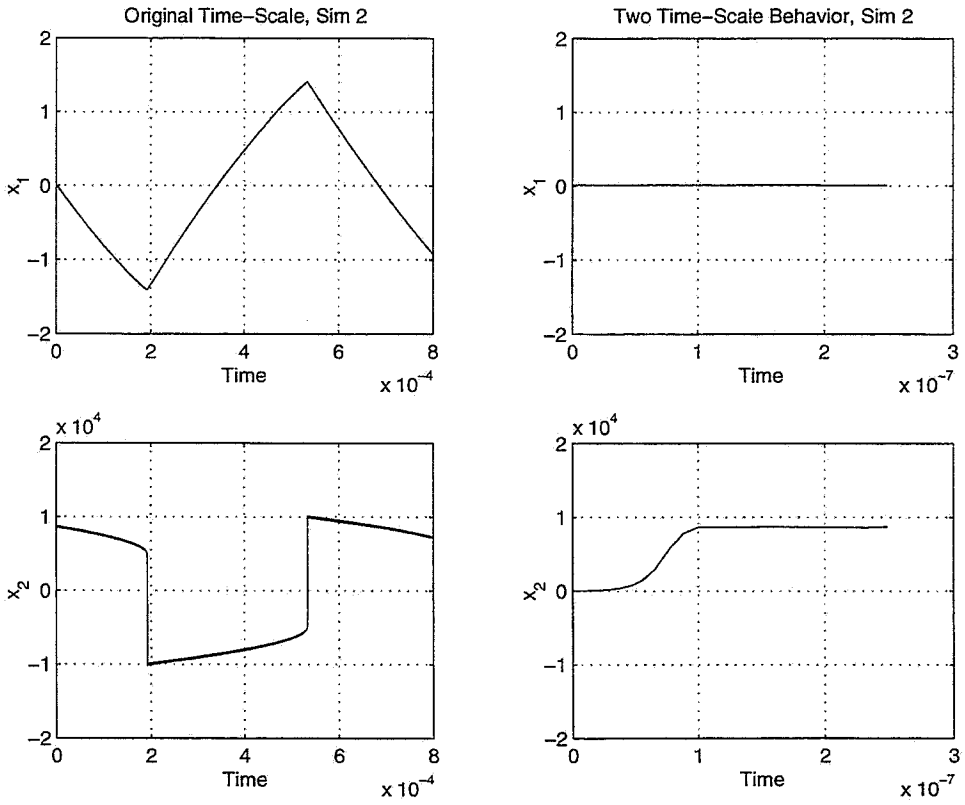

Figure 6: Simulation 2. Two time-scale behavior for $\varepsilon = 1.0 \times 10^{-9}$.

Our third and final simulation used the following values for the parameters:

$$q_2 = 1$$

$$p(\varepsilon) = \varepsilon, \qquad c = 1,$$

which correspond to Case 2 in Table 1. The value for n is now $\frac{3}{2}$ which is again larger than the prescribed maximum of $\frac{4}{3}$. As shown in Figure 7(a), the stability region contracts along the x_1-axis while it continuously expands along the x_2-axis. The stability region is narrow along the x_1-axis and shows no signs of expanding along that direction, so any perturbation of the initial condition for x_1 greater than approximately 0.4 would cause the system response to be unbounded.

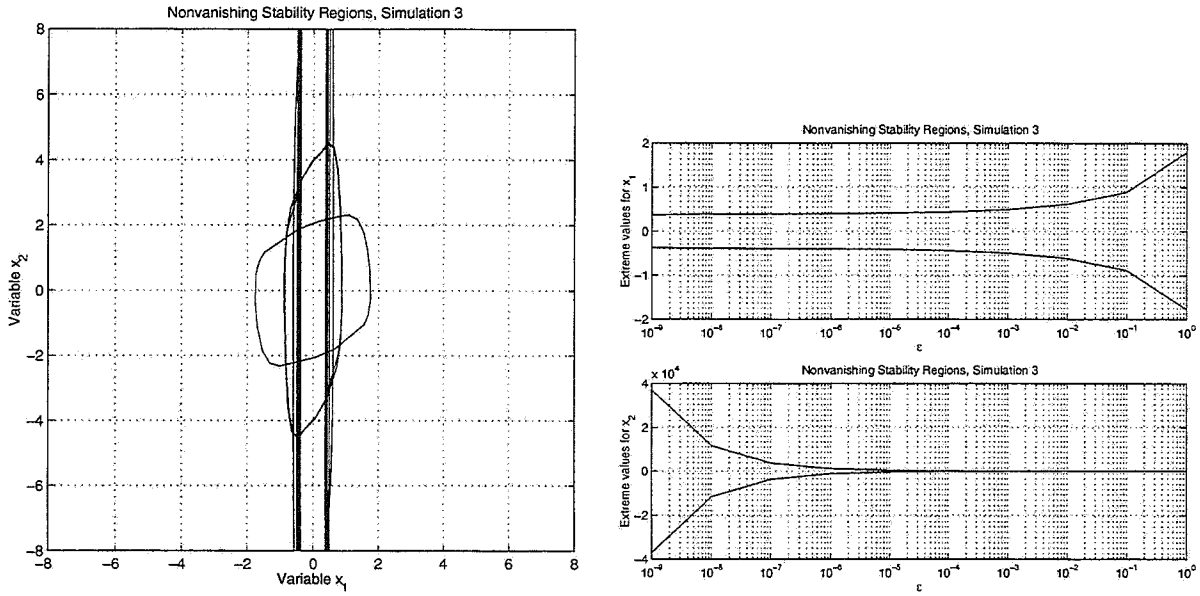

(a) (b)

Figure 7: Simulation 3. Parameter values: $q_2 = 1$, $p(\varepsilon) = \varepsilon$, and $n = \frac{3}{2}$. Part (a) shows the simulated stability region boundary as the value of ε decreases. Part (b) plots the extreme values for state variables x_1 and x_2 versus ε.

As before, we also present Table 5 and Figures 8 and 9 to allow for a complete comparison among the simulations.

Our three simulations illustrate the results of Sections 2 and 3 and demonstrate how condition (52) allows us to construct linear feedback controllers using an H^∞ approach and still maintain the stability regions. These numerical results verify our analysis and deliver the expected behavior for the parameters we studied.

5 Conclusion

We analyzed a second-order system with nonlinear disturbance terms and derived a sufficient condition on the design parameters to ensure that the stability region would not vanish as the feedback gains increased. We were interested in the high-gain case because we considered the asymptotically optimal H^∞ design approach to the problem. Using this technique, as we allowed the disturbance attenuation level to approach the optimal value and the cost on control to become cheap, the feedback gains increased to infinity. We manipulated the attenuation level and the control cost because both terms play a role in determining the magnitude of the feedback. The rate at which the two terms approach their limits determines which plays the dominant role in computing the feedback gains for the six cases we examined. Previous results showed that such high-gain feedback could lead to vanishing stability regions if the disturbance terms contained

Table 5: Simulation 3 numerical results. The table contains the absolute value of each quantity to simplify comparisons.

ε	$p(\varepsilon)$	γ^{*2}	k_1	k_2	λ_1	λ_2
1.00e+00	1.00e+00	2.00e+00	3.00e+00	3.87e+00	2.80e+00	1.07e+00
1.00e-01	1.00e-01	1.01e+00	4.48e+01	1.45e+01	9.99e+00	4.48e+00
1.00e-02	1.00e-02	1.00e+00	1.11e+03	1.11e+02	1.00e+02	1.11e+01
1.00e-03	1.00e-03	1.00e+00	3.27e+04	1.03e+03	1.00e+03	3.27e+01
1.00e-04	1.00e-04	1.00e+00	1.01e+06	1.01e+04	1.00e+04	1.01e+02
1.00e-05	1.00e-05	1.00e+00	3.17e+07	1.00e+05	1.00e+05	3.17e+02
1.00e-06	1.00e-06	1.00e+00	1.00e+09	1.00e+06	1.00e+06	1.00e+03
1.00e-07	1.00e-07	1.00e+00	3.16e+10	1.00e+07	1.00e+07	3.16e+03
1.00e-08	1.00e-08	1.00e+00	1.00e+12	1.00e+08	1.00e+08	1.00e+04
1.00e-09	1.00e-09	1.00e+00	3.28e+13	1.00e+09	1.00e+09	3.28e+04

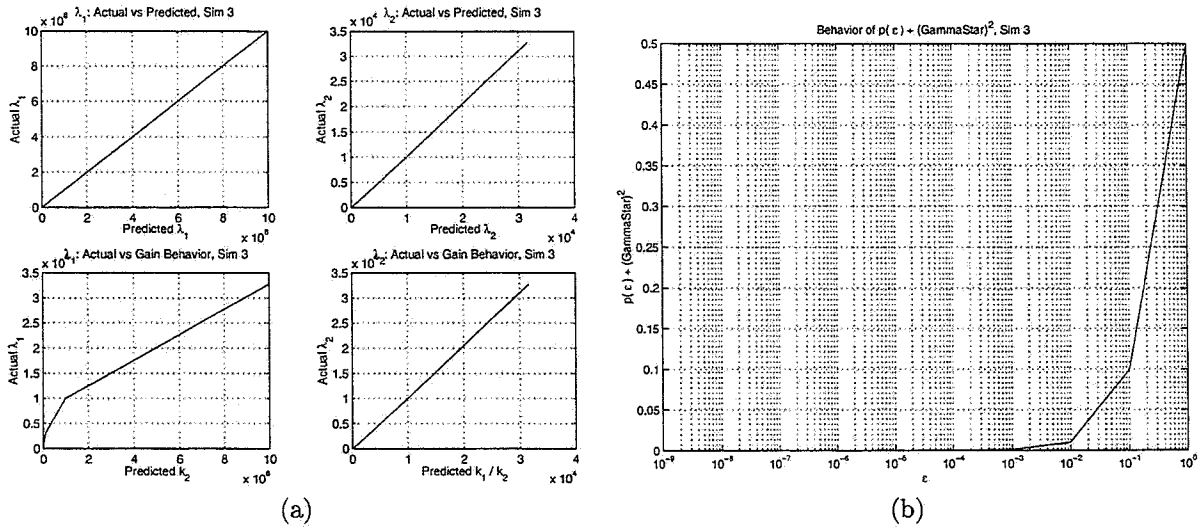

(a) (b)

Figure 8: Simulation 3. Part (a) eigenvalue relationships as ε varies. Part (b) behavior of $p(\varepsilon)/\gamma^{*2}$ as $\varepsilon \to 0$.

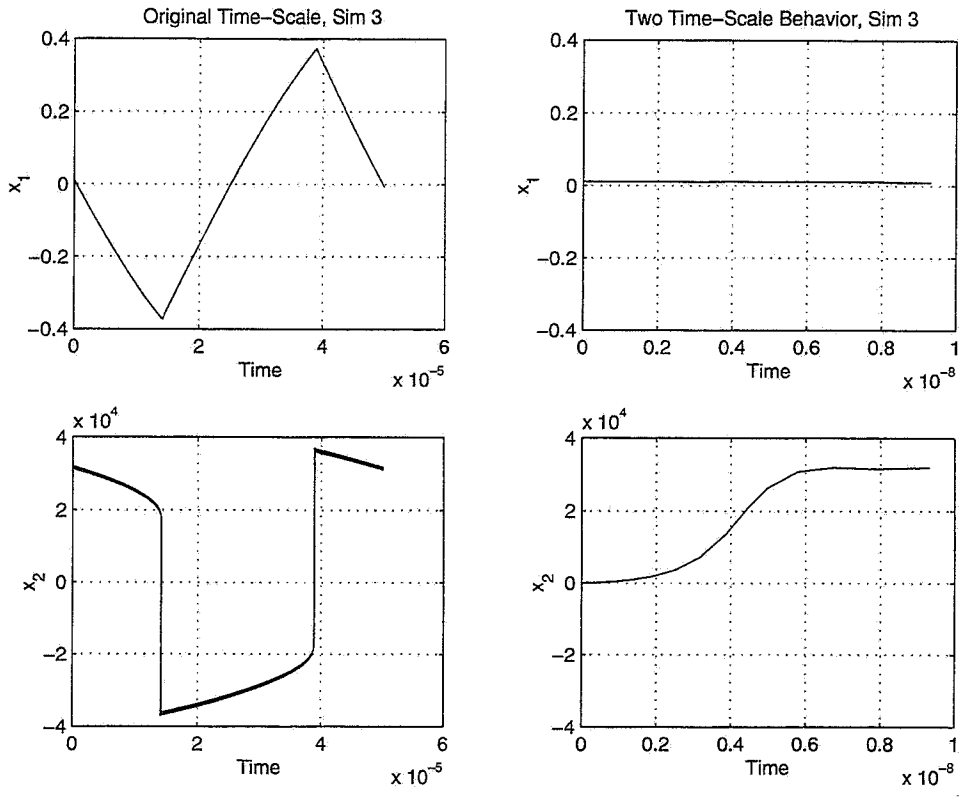

Figure 9: Simulation 3. Two time-scale behavior for $\varepsilon = 1.0 \times 10^{-9}$.

nonlinearities. To prevent the stability region from vanishing, we first determined the relationship between the design parameters and feedback gains. We then applied a Lyapunov-based analysis to determine a sufficient condition on the design parameters to prevent the stability region from vanishing. We described three simulations that illustrate and verify our design method. Our approach is unique because it considered the asymptotically optimal H^∞ design for the controller and offers the optimal solution with respect to a given performance measure.

There are several avenues of research that start where we leave off. One direction could be to find a simplified version of the stability proof offered in Section 3. We found one approach using Lyapunov theory, but there may be other more elegant solutions to the current problem. Our analysis offers only a sufficient condition for stability, so a proof that develops necessary conditions would be a second valuable extension.

A third challenging problem is to extend the results to higher-order systems. Preliminary simulations show that the stability region for a simple third-order system can vanish as the feedback gains increase. However, fully analyzing this system is significantly more difficult than the second order case presented here. The essential step to extending the results is to find an analytical expression for the Z matrix solving the algebraic Riccati equations. Numerical solutions will not be adequate for a rigorous proof and the analytical solution is quite difficult. One tactic may be to use a derivation based on behavior of the entries in Z in the limit as the matrix approaches the minimal solution. We expect this type of approach to be similar to the analyses of systems with multiple time-scale behavior. Another approach could be to use a backstepping inspired technique where the results from a higher-order system are simplified by removing one dimension at a time [18, 11]. Finally, the techniques from [16, 17] offer another option for resolving the extension to higher-order systems. Solving the nonvanishing stability regions problem associated with optimal H^∞ control for third- and higher-order systems remains an open and challenging research problem.

6 Acknowledgment

We wish to acknowledge discussions with and contributions of Scott Splater, Zigang Pan, and Petar V. Kokotović at the earlier stages of this research.

A Limiting Behavior of $p(\varepsilon)$ versus γ^{*2}

We demonstrate that for the six cases of interest, the condition

$$\lim_{\varepsilon \to 0} \frac{p(\varepsilon)}{\gamma^{*2}} = 0$$

always holds. Before we present the details for each case, we observe that a Taylor's series expansion of γ^{*2} as a function of ε is

$$\gamma^{*2}(\varepsilon) = q_2 + \frac{q_1}{q_2}\varepsilon^2 + O(\varepsilon^2).$$

The derivation for this expression is given in Appendix B.

A.1 Case 1 and Case 2

The parameter settings are

$$\begin{aligned} q_2 &> 0, \quad \text{constant} \\ p(\varepsilon) &= \varepsilon^c, \qquad c > 2 \quad \text{(Case 1)}; \qquad c < 2 \quad \text{(Case 2)}. \end{aligned}$$

We start with the original condition, apply the Taylor's series expansion and take the limit to get the results.

$$\lim_{\varepsilon \to 0} \frac{p(\varepsilon)}{\gamma^{*2}} = \lim_{\varepsilon \to 0} \left[\frac{\varepsilon^c}{q_2 + \frac{q_1}{q_2}\varepsilon^2 + O(\varepsilon^2)} \right] = \frac{0}{q_2} = 0.$$

A.2 Case 3

The parameter settings are

$$\begin{aligned} q_2 &= 0, \qquad \text{constant} \\ p(\varepsilon) &= \varepsilon^{1+c}, \qquad c > 0. \end{aligned}$$

The limit condition is

$$\begin{aligned} \lim_{\varepsilon \to 0} \frac{p(\varepsilon)}{\gamma^{*2}} &= \lim_{\varepsilon \to 0} \left[\frac{\varepsilon^{1+c}}{0 + \frac{q_1}{q_2}\varepsilon^2 + O(\varepsilon^2)} \right] \\ &= \lim_{\varepsilon \to 0} \left[\frac{q_2\, \varepsilon^{1+c}}{q_1\, \varepsilon^2 + q_2\, O(\varepsilon^2)} \right] = \lim_{\varepsilon \to 0} \frac{0}{q_1\, \varepsilon^2} = 0. \end{aligned}$$

A.3 Case 4 and Case 5

The parameter settings are

$$\begin{aligned} q_2 &= \varepsilon^l, \qquad 0 < l < 1 \\ p(\varepsilon) &= \varepsilon^{l+c}, \qquad c > 2 - 2l \quad \text{(Case 4)}; \qquad c < 2 - 2l \quad \text{(Case 5)}. \end{aligned}$$

The limit condition is

$$\lim_{\varepsilon\to 0}\frac{p(\varepsilon)}{\gamma^{*2}} = \lim_{\varepsilon\to 0}\left[\frac{\varepsilon^{l+c}}{q_2+\frac{q_1}{q_2}\varepsilon^2+O(\varepsilon^2)}\right]$$
$$= \lim_{\varepsilon\to 0}\left[\frac{\varepsilon^{l+c}}{\varepsilon^l+q_1\,\varepsilon^{2-l}+O(\varepsilon^2)}\right] = \frac{\varepsilon^{l+c}}{\varepsilon^l} = 0.$$

A.4 Case 6

The parameter settings are

$$q_2 = \varepsilon^l, \qquad 1\le l$$
$$p(\varepsilon) = \varepsilon^{1+c}, \qquad c>0.$$

The limit condition is

$$\lim_{\varepsilon\to 0}\frac{p(\varepsilon)}{\gamma^{*2}} = \lim_{\varepsilon\to 0}\left[\frac{\varepsilon^{1+c}}{q_2+\frac{q_1}{q_2}\varepsilon^2+O(\varepsilon^2)}\right]$$
$$= \lim_{\varepsilon\to 0}\left[\frac{\varepsilon^{1+c}}{\varepsilon^l+q_1\,\varepsilon^{2-l}+O(\varepsilon^2)}\right] = \frac{\varepsilon^{l+c}}{q_1\,\varepsilon^{2-l}} = 0.$$

B Derivation of Z Matrix Values

This appendix outlines the derivations we used to compute the Z matrix values in Section 2. We analyzed six cases and will provide the complete derivation for the first case. For the other five cases, we will outline the key steps and skip some of the details. The Z matrix has the form

$$Z = \begin{pmatrix} z_{11} & z_{12} \\ z_{12} & z_{22}\end{pmatrix},$$

and we recall

$$\beta_1 = \frac{1}{\gamma^2}, \quad \beta_2 = \frac{\gamma^2-\varepsilon^2}{\gamma^2\varepsilon^2},$$

from Section 2. For convenience, we rewrite here the formulas for the elements of the Z matrix also presented in Section 2

$$z_{11} = \left(\frac{\beta_2\,z_{12}^2-q_1}{\beta_1}\right)^{\frac{1}{2}}, \quad z_{22} = \left(\frac{q_2+2z_{12}+\beta_1\,z_{12}^2}{\beta_2}\right)^{\frac{1}{2}} \tag{60}$$

with

$$z_{12} = \frac{\gamma^2\,\varepsilon\left[q_1\,\varepsilon+\left(q_1\left[\gamma^2-q_2\right]\left[\gamma^2-\varepsilon^2\right]\right)^{\frac{1}{2}}\right]}{\gamma^4-(q_2+\varepsilon^2)\,\gamma^2+(q_2-q_1)\,\varepsilon^2}. \tag{61}$$

Finally, we will refer to the expression for γ^{*2}, computed from (12) as

$$\gamma^{*2} = \frac{1}{2}\left[q_2+\varepsilon^2+(q_2^2-2q_2\,\varepsilon^2+\varepsilon^4+4q_1\,\varepsilon^2)^{\frac{1}{2}}\right], \tag{62}$$

along with its relationship to γ^2

$$\gamma^2 = \gamma^{*2}+p(\varepsilon). \tag{63}$$

With these universal equations stated, we are now prepared to complete the derivations.

B.1 Case 1

Case 1 corresponds to q_2 as a positive constant and $p(\varepsilon) = \varepsilon^c$ with $c > 2$. As ε approaches zero, from (62), we see γ^{*2} approaches

$$\lim_{\varepsilon \to 0} \gamma^{*2} = \frac{1}{2}\left[q_2 + \sqrt{q_2^2}\right] = q_2.$$

To make γ approach γ^*, we need

$$\lim_{\varepsilon \to 0} p(\varepsilon) = \lim_{\varepsilon \to 0} \varepsilon^c = 0,$$

so we require that $c > 0$. As ε approaches zero, the denominator of z_{12} (abbreviated as $\mathrm{Den}(z_{12})$) approaches $q_2\, p(\varepsilon)$ as shown below

$$\begin{aligned}
\mathrm{Den}(z_{12}) &= \gamma^4 - (q_2 + \varepsilon^2)\gamma^2 + (q_2 - q_1)\varepsilon^2 \\
\mathrm{Den}(z_{12}) &= \left[\gamma^{*2} + p(\varepsilon)\right]^2 - (q_2 + \varepsilon^2)\left[\gamma^{*2} + p(\varepsilon)\right] + (q_2 - q_1)\varepsilon^2 \\
\lim_{\varepsilon \to 0} \mathrm{Den}(z_{12}) &\sim \left[\gamma^{*2} + p(\varepsilon)\right]^2 - q_2\left[\gamma^{*2} + p(\varepsilon)\right] \\
&\sim \gamma^{*4} + 2\gamma^{*2} p(\varepsilon) + \underbrace{p^2(\varepsilon)}_{\to 0} - q_2\gamma^{*2} - q_2\, p(\varepsilon) \\
&\sim q_2^2 + 2q_2\, p(\varepsilon) - q_2^2 - q_2\, p(\varepsilon) \sim q_2\, p(\varepsilon).
\end{aligned}$$

To find a valid nonzero expression for the numerator of z_{12} (abbreviated as $\mathrm{Num}(z_{12})$) we need to find a Taylor series expansion of γ^{*2} around zero. Consider γ^* as a function of ε and write $\gamma^{*2}(\varepsilon)$ as in (62). We note that $\gamma^{*2}(0) = \frac{1}{2}\left[q_2 + \sqrt{q_2^2}\right] = q_2$. Now compute the first two derivatives of $\gamma^{*2}(\varepsilon)$ and evaluate them at zero as shown below.

$$\begin{aligned}
\frac{d\gamma^{*2}(0)}{d\varepsilon} &= \frac{1}{2}\left[2\varepsilon + \frac{1}{2}(q_2^2 - 2q_2\varepsilon^2 + \varepsilon^4 + 4q_1\varepsilon^2)^{-\frac{1}{2}}(-4q_2\varepsilon + 4\varepsilon^3 + 8q_1\varepsilon)\right]\Big|_{\varepsilon=0} \\
&= 0, \\
\frac{d^2\gamma^{*2}(0)}{d\varepsilon^2} &= \left[1 + (-\frac{1}{8})(q_2^2 - 2q_2\varepsilon^2 + \varepsilon^4 + 4q_1\varepsilon^2)^{-\frac{3}{2}}(-4q_2\varepsilon + 4\varepsilon^3 + 8q_1\varepsilon)^2\right. \\
&\quad \left. + \frac{1}{4}(q_2^2 - 2q_2\varepsilon^2 + \varepsilon^4 + 4q_1\varepsilon^2)^{-\frac{1}{2}}(-4q_2 + 12\varepsilon^2 + 8q_1)\right]\Big|_{\varepsilon=0} \\
&= 1 + \frac{1}{4}(q_2^2)^{-\frac{1}{2}}(-4q_2 + 8q_1) = 1 + \frac{1}{4q_2}(-4q_2 + 8q_1) = 1 - 1 + \frac{2q_1}{q_2} = \frac{2q_1}{q_2}.
\end{aligned}$$

So now writing γ^{*2} as a Taylor's series we get

$$\begin{aligned}
\gamma^{*2}(\varepsilon) &= q_2 + 0 + \frac{1}{2}\frac{2q_1}{q_2}\varepsilon^2 + O(\varepsilon^2) \\
&= q_2 + \frac{q_1}{q_2}\varepsilon^2 + O(\varepsilon^2).
\end{aligned}$$

Now we can derive an expression for the numerator of z_{12} as follows:

$$\begin{aligned}
\text{Num}(z_{12}) &= \gamma^2\,\varepsilon\left[q_1\,\varepsilon + \left(q_1\left[\gamma^2 - q_2\right]\left[\gamma^2 - \varepsilon^2\right]\right)^{\frac{1}{2}}\right] \\
&= \varepsilon\left[\gamma^{*2} + p(\varepsilon)\right]\left[q_1\,\varepsilon + \left(q_1\left[\gamma^{*2} + p(\varepsilon) - q_2\right]\left[\gamma^{*2} + p(\varepsilon) - \varepsilon^2\right]\right)^{\frac{1}{2}}\right] \\
&= \varepsilon\left(q_2 + \frac{q_1}{q_2}\,\varepsilon^2 + O(\varepsilon^2) + p(\varepsilon)\right) \\
&\quad \times \left\{q_1\,\varepsilon + \left(q_1\left[q_2 + \frac{q_1}{q_2}\,\varepsilon^2 + O(\varepsilon^2) + p(\varepsilon) - q_2\right]\right.\right. \\
&\quad \left.\left. \times \left[q_2 + \frac{q_1}{q_2}\,\varepsilon^2 + O(\varepsilon^2) + p(\varepsilon) - \varepsilon^2\right]\right)^{\frac{1}{2}}\right\} \\
\lim_{\varepsilon\to 0}\text{Num}(z_{12}) &\sim \varepsilon\,q_2\left[q_1\,\varepsilon + \left(q_1\left[\frac{q_1}{q_2}\,\varepsilon^2\right]\left[q_2\right]\right)^{\frac{1}{2}}\right] \\
&\sim \varepsilon\,q_2\left[q_1\,\varepsilon + \left(q_1^2\,\varepsilon^2\right)^{\frac{1}{2}}\right] \sim \varepsilon\,q_2\left[q_1\,\varepsilon + q_1\,\varepsilon\right] \sim 2q_1\,q_2\,\varepsilon^2.
\end{aligned}$$

Now we combine the denominator and numerator expressions to get

$$z_{12} \sim \frac{2q_1\,q_2\,\varepsilon^2}{q_2\,p(\varepsilon)} \sim \frac{2q_1\,\varepsilon^2}{p(\varepsilon)}.$$

We can now use z_{12} to find similar expressions for z_{11} and z_{22} using (60). We will need the expression for z_{12}^2

$$z_{12}^2 = \frac{4q_1^2\,\varepsilon^4}{p^2(\varepsilon)}.$$

Now solve for z_{11}

$$\begin{aligned}
z_{11} &= \left[\frac{\beta_2\,z_{12}^2 - q_1}{\beta_1}\right]^{\frac{1}{2}} = \left[\frac{\left(\frac{\gamma^2-\varepsilon^2}{\gamma^2\varepsilon^2}\right)\left(\frac{4q_1^2\,\varepsilon^4}{p^2(\varepsilon)}\right) - q_1}{\frac{1}{\gamma^2}}\right]^{\frac{1}{2}} \\
&= \left[\left(\gamma^2 - \varepsilon^2\right)\left(\frac{4q_1^2\,\varepsilon^2}{p^2(\varepsilon)}\right) - \gamma^2\,q_1\right]^{\frac{1}{2}} = \left[\frac{4\gamma^2\,q_1^2\,\varepsilon^2 - 4q_1^2\,\varepsilon^4 - \gamma^2\,q_1\,p^2(\varepsilon)}{p^2(\varepsilon)}\right]^{\frac{1}{2}} \\
\lim_{\varepsilon\to 0} z_{11} &\sim \left[\frac{4\gamma^2\,q_1^2\,\varepsilon^2}{p^2(\varepsilon)}\right]^{\frac{1}{2}} \sim \left[\frac{4q_2\,q_1^2\,\varepsilon^2}{p^2(\varepsilon)}\right]^{\frac{1}{2}} \sim \frac{2q_1\,\varepsilon\sqrt{q_2}}{p(\varepsilon)}.
\end{aligned}$$

Similarly solve for z_{22}

$$\begin{aligned}
z_{22} &= \left[\frac{q_2 + 2z_{12} + \beta_1\,z_{12}^2}{\beta_2}\right]^{\frac{1}{2}} = \left[\frac{q_2 + \frac{4q_1\,\varepsilon^2}{p(\varepsilon)} + \frac{4q_1^2\,\varepsilon^4}{\gamma^2\,p^2(\varepsilon)}}{\frac{\gamma^2-\varepsilon^2}{\gamma^2\varepsilon^2}}\right]^{\frac{1}{2}} \\
&= \left[\left(\frac{\gamma^2\varepsilon^2}{\gamma^2 - \varepsilon^2}\right)\left(\frac{\gamma^2\,p^2(\varepsilon)\,q_2 + 4\gamma^2\,p(\varepsilon)\,q_1\,\varepsilon^2 + 4q_1^2\,\varepsilon^4}{\gamma^2 p^2(\varepsilon)}\right)\right]^{\frac{1}{2}} \\
\lim_{\varepsilon\to 0} z_{22} &\sim \left[\frac{4q_1^2\,\varepsilon^6}{\gamma^2\,p^2(\varepsilon)}\right]^{\frac{1}{2}} \sim \frac{2q_1\,\varepsilon^3}{p(\varepsilon)\sqrt{q_2}}.
\end{aligned}$$

With these derivations, we can now return to Section 2 and follow the rest of the analysis for Case 1 starting with (15). For completeness, we included all of the constants in this derivation to make the steps easier to follow. For simplicity, we will eliminate the constants in the remaining derivations below.

B.2 Case 2

For the second case and those that follow, we will state the main results similar to those given for Case 1. Case 2 corresponds to q_2 as a positive constant and $p(\varepsilon) = \varepsilon^c$ with $c < 2$. We note that the expression for z_{11} is not required to compute the expressions for the feedback gains or the eigenvalues so we will omit z_{11} from now on. Also recall the following relationships from Section 2:

$$\begin{aligned} k_1 &= \tfrac{1}{\varepsilon^2} z_{12} & k_2 &= \tfrac{1}{\varepsilon^2} z_{22} \\ \lambda_1 &\sim k_2 & \lambda_2 &\sim \tfrac{k_1}{k_2} \\ n &= \tfrac{\log_\varepsilon k_1}{\log_\varepsilon k_2}. \end{aligned}$$

The results for Case 2 are

$$\begin{aligned} \mathrm{Den}(z_{12}) &\sim p(\varepsilon) & \mathrm{Num}(z_{12}) &\sim \varepsilon\sqrt{p(\varepsilon)} \\ z_{12} &\sim \tfrac{\varepsilon}{\sqrt{p(\varepsilon)}} & z_{22} &\sim \varepsilon \\ k_1 &\sim \tfrac{1}{\varepsilon\sqrt{p(\varepsilon)}} & k_2 &\sim \tfrac{1}{\varepsilon} \\ \lambda_1 &\sim \tfrac{1}{\varepsilon} & \lambda_2 &\sim \tfrac{1}{\sqrt{p(\varepsilon)}} \\ n &= 1 + \tfrac{c}{2}. \end{aligned}$$

B.3 Case 3

Case 3 corresponds to q_2 set to zero and $p(\varepsilon) = \varepsilon^{1+c}$ with $c > 0$. The results for Case 3 are

$$\begin{aligned} \mathrm{Den}(z_{12}) &\sim \varepsilon^{2+c} & \mathrm{Num}(z_{12}) &\sim \varepsilon^3 \\ z_{12} &\sim \varepsilon^{1-c} & z_{22} &\sim \varepsilon^{\frac{3}{2}-c} \\ k_1 &\sim \varepsilon^{-1-c} & k_2 &\sim \varepsilon^{-\frac{1}{2}-c} \\ \lambda_1 &\sim \tfrac{\sqrt{\varepsilon}}{p(\varepsilon)} & \lambda_2 &\sim \tfrac{1}{\sqrt{\varepsilon}} \\ n &= \tfrac{2c+2}{2c+1}. \end{aligned}$$

B.4 Case 4

Case 4 corresponds to $q_2 = \varepsilon^l$ with $0 < l < 1$ and $p(\varepsilon) = \varepsilon^{l+c}$ and with $c > 2 - 2l$. The results for Case 4 are

$$\begin{aligned} \mathrm{Den}(z_{12}) &\sim \varepsilon^{2l+c} & \mathrm{Num}(z_{12}) &\sim \varepsilon^{2+l} \\ z_{12} &\sim \varepsilon^{2-l-c} & z_{22} &\sim \varepsilon^{3-\frac{3}{2}l-c} \\ k_1 &\sim \varepsilon^{-l-c} & k_2 &\sim \varepsilon^{1-\frac{3}{2}l-c} \\ \lambda_1 &\sim \tfrac{\varepsilon^{(1-\frac{1}{2}l)}}{p(\varepsilon)} & \lambda_2 &\sim \tfrac{1}{\varepsilon^{(1-\frac{1}{2}l)}} \\ n &= \tfrac{2(l+c)}{3l+2c-2}. \end{aligned}$$

B.5 Case 5

Case 5 corresponds to $q_2 = \varepsilon^l$ with $0 < l < 1$ and $p(\varepsilon) = \varepsilon^{l+c}$ and with $c < 2 - 2l$. The results for Case 5 are

$$\begin{aligned} \text{Den}(z_{12}) &\sim \varepsilon^{2l+c} & \text{Num}(z_{12}) &\sim \varepsilon^{1+2l+\frac{1}{2}c} \\ z_{12} &\sim \varepsilon^{1-\frac{1}{2}c} & z_{22} &\sim \varepsilon^{1+\frac{1}{2}l} \\ k_1 &\sim \varepsilon^{-1-\frac{1}{2}c} & k_2 &\sim \varepsilon^{-1+\frac{1}{2}l} \\ \lambda_1 &\sim \frac{1}{\varepsilon^{(1-\frac{1}{2}l)}} & \lambda_2 &\sim \frac{1}{\sqrt{p(\varepsilon)}} \\ n &= \frac{c+2}{2-l}. \end{aligned}$$

B.6 Case 6

Case 6 corresponds to $q_2 = \varepsilon^l$ with $1 \leq l$ and $p(\varepsilon) = \varepsilon^{1+c}$ with $c > 0$. The results for Case 6 are

$$\begin{aligned} \text{Den}(z_{12}) &\sim \varepsilon^{2+c} & \text{Num}(z_{12}) &\sim \varepsilon^{3} \\ z_{12} &\sim \varepsilon^{1-c} & z_{22} &\sim \varepsilon^{\frac{3}{2}-c} \\ k_1 &\sim \varepsilon^{-1-c} & k_2 &\sim \varepsilon^{-\frac{1}{2}-c} \\ \lambda_1 &\sim \frac{\sqrt{\varepsilon}}{p(\varepsilon)} & \lambda_2 &\sim \frac{1}{\sqrt{\varepsilon}} \\ n &= \frac{2c+2}{2c+1}. \end{aligned}$$

C Derivation of Conditions on Parameter c

This appendix provides the details on translating condition (52) into a condition on the c parameter. The results for Case 1 from Section 3 are repeated here along with the other five cases. Each derivation begins with (52), which is restated here for convenience:

$$n < 1 + \frac{1}{2\nu - 3}, \qquad \nu > 2. \tag{64}$$

C.1 Case 1

$$n = \frac{c}{c-1}$$

$$\frac{c}{c-1} < 1 + \frac{1}{2\nu-3} \iff c < \frac{(2\nu-2)(c-1)}{2\nu-3}$$

$$\iff \left[1 - \left(\frac{2\nu-2}{2\nu-3}\right)\right] c < \frac{2-2\nu}{2\nu-3} \iff \frac{-1}{2\nu-3} c < \frac{2-2\nu}{2\nu-3} \iff c > 2\nu - 2$$

C.2 Case 2

$$n = 1 + \frac{c}{2}$$

$$1 + \frac{c}{2} < \frac{2\nu-2}{2\nu-3} \iff \frac{c}{2} < \frac{1}{2\nu-3} \iff c < \frac{2}{2\nu-3}$$

C.3 Case 3

$$n = \frac{2c+2}{2c+1}$$

$$\frac{c+1}{c+\frac{1}{2}} < \frac{2\nu-2}{2\nu-3} \iff c+1 < c\left(\frac{2\nu-2}{2\nu-3}\right) + \frac{\nu-1}{2\nu-3}$$

$$\iff \left[1-\left(\frac{2\nu-2}{2\nu-3}\right)\right]c < \frac{\nu-1}{2\nu-3} - 1 \iff \left[-\frac{1}{2\nu-3}\right]c < \frac{2-\nu}{2\nu-3} \iff c > \nu-2$$

C.4 Case 4

$$n = \frac{2(l+c)}{3l+2c-2}$$

$$\frac{-l-c}{1-\frac{3}{2}l-c} < \frac{2\nu-2}{2\nu-3}$$

$$\iff -l-c > \left(\frac{2\nu-2}{2\nu-3}\right)\left(1-\frac{3}{2}l-c\right)$$

$$\iff -l-c > -c\left(\frac{2\nu-2}{2\nu-3}\right) + \left(1-\frac{3}{2}l\right)\left(\frac{2\nu-2}{2\nu-3}\right)$$

$$\iff \left[\left(\frac{2\nu-2}{2\nu-3}\right)-1\right]c > l + \left(1-\frac{3}{2}l\right)\left(\frac{2\nu-2}{2\nu-3}\right)$$

$$\iff \left[\frac{2\nu-2-2\nu+3}{2\nu-3}\right]c > \frac{1}{2\nu-3}\left[l(2\nu-3) + \left(1-\frac{3}{2}l\right)(2\nu-2)\right]$$

$$\iff c > 2l\nu - 3l + 2\nu - 2 - 3l\nu + 3l \iff c > 2\nu - l\nu - 2 \iff c > \nu(2-l) - 2$$

C.5 Case 5

$$n = \frac{c+2}{2-l}$$

$$\frac{c+2}{2-l} < \frac{2\nu-2}{2\nu-3} \iff c+2 < \frac{1}{2\nu-3}(4\nu - 2\nu l - 4 + 2l)$$

$$\iff c < \frac{1}{2\nu-3}(4\nu - 2\nu l - 4 + 2l - 4\nu + 6) \iff c < \frac{1}{2\nu-3}(2 + 2l - 2\nu l) \iff c < \frac{2+2l(1-\nu)}{2\nu-3}$$

C.6 Case 6

$$n = \frac{2c+2}{2c+1}$$

$$\frac{c+1}{c+\frac{1}{2}} < \frac{2\nu-2}{2\nu-3} \iff c+1 < c\left(\frac{2\nu-2}{2\nu-3}\right) + \frac{\nu-1}{2\nu-3}$$

$$\iff \left[1-\left(\frac{2\nu-2}{2\nu-3}\right)\right]c < \frac{\nu-1}{2\nu-3} - 1 \iff \left[-\frac{1}{2\nu-3}\right]c < \frac{2-\nu}{2\nu-3} \iff c > \nu-2$$

References

[1] H. D. Chiang and J. S. Thorp. Stability regions of nonlinear dynamical systems: a constructive methodology. *IEEE Trans. on Auto. Contr.*, 34(12):1229–1241, 1989.

[2] R. Genesio, M. Tartaglia, and A. Vicino. On the estimation of asymptotic stability regions: State of the art and new proposals. *IEEE Trans. on Auto. Contr.*, 30(8):747–755, 1985.

[3] R. Genesio and A. Vicino. New techniques for constructing asymptotic stability regions for nonlinear systems. *IEEE Trans. on Cir. & Sys*, 31:574–581, 1984.

[4] H. D. Chiang and A. L. Fekih. A constructive methodology for estimating the stability regions of interconnected nonlinear system. *IEEE Trans. on Cir. & Sys*, 37(5):577–588, 1990.

[5] H. D. Chiang, M. W. Hirsch, and F. F. Wu. Stability regions of nonlinear autonomous dynamical systems. *IEEE Trans. on Auto. Contr.*, 33(1):16–27, 1988.

[6] H. D. Chiang and A. L. Fekih. Quasi-stability regions of nonlinear dynamical systems: theory. *IEEE Transactions on Circuits and Systems: Part I*, 43(8):627–635, 1996.

[7] T. Başar and P. Bernhard. *H^∞-Optimal Control and Related Minimax Design Problems.* Birkhäuser, Boston, Second edition, 1995.

[8] P. V. Kokotović and R. Marino. On vanishing stability regions in nonlinear systems with high-gain feedback. *IEEE Trans. on Auto. Contr.*, 31(10):967–970, 1986.

[9] B. dAndrea and J. Levine. Nonlinear control and high gain approaches for the control of a robot arm: new results and comparisons. In *Automatic Control - World Congress, 1987. Selected Papers from the 10th Triennial World Congress of the International Federation of Automatic Control*, volume 4, pages 295–300. IFAC, 1988.

[10] A. Teel and L. Praly. Tools for semiglobal stabilization by partial state and output feedback. *SIAM J. Contr. and Opt.*, 33(5):1443–1488, 1995.

[11] M. Krstić, J. Sun, and P. V. Kokotović. Robust control of nonlinear systems with input unmodeled dynamics. *IEEE Trans. on Auto. Contr.*, 41(6):913–920, 1996.

[12] J. H. Chow and P. V. Kokotović. A decomposition of near-optimum regulators for systems with slow and fast modes. *IEEE Trans. on Auto. Contr.*, 21:701–705, 1976.

[13] A. Saberi and H. Khalil. Stabilization and regulation of nonlinear singularly perturbed systems—composite control. *IEEE Trans. on Auto. Contr.*, 30(8):739–747, 1985.

[14] H. K. Khalil. Stability analysis of nonlinear multiparameter singularly perturbed systems. *IEEE Trans. on Auto. Contr.*, 32(3):260–263, 1987.

[15] K. W. Cheung and J. H. Chow. Stability analysis of singularly perturbed systems using slow and fast manifolds. In *Proceedings of the 1991 American Control Conference*, volume 2, pages 1685–1690. IEEE, 1991.

[16] Z. Pan and T. Başar. H^∞-optimal control for singularly perturbed systems. Part I: Perfect state measurements. *Automatica*, 29(2):401–423, 1993.

[17] Z. Pan and T. Başar. Time-scale separation and robust controller design for uncertain nonlinear singularly perturbed systems under perfect state measurements. *International Journal of Robust and Nonlinear Control*, 6:585–608, 1996.

[18] H. K. Khalil. *Nonlinear Systems.* Prentice Hall, Upper Saddle River, NJ, Second edition, 1996.

[19] A. Isidori. *Nonlinear Control Systems.* Springer, Great Britain, Third edition, 1995.